[AMERICAN JOURNAL OF SCIENCE, VOL. 287, JUNE, 1987, P. 517-559]

American Journal of Science

JUNE 1987

THE REACTION MUSCOVITE + QUARTZ ⇄ ANDALUSITE + K-FELDSPAR + WATER. PART 1. GROWTH KINETICS AND MECHANISM

JANET A. SCHRAMKE*, DERRILL M. KERRICK, and ANTONIO C. LASAGA**

Department of Geosciences, The Pennsylvania State University, University Park, Pennsylvania 16802

ABSTRACT. The growth kinetics and mechanism of the metamorphic reaction muscovite + quartz ⇄ andalusite + sanidine + water were investigated from 0.5 to 5 kb and from 350° to 700°C in the presence of a pure aqueous fluid. Examination of run products with a scanning electron microscope (SEM) established that the hydration and dehydration reactions took place through a dissolution–transport–precipitation mechanism. Dependence of the reaction rates on andalusite surface area, textural features of run products, low calculated concentration gradients in the aqueous phase, and calculated values of the apparent activation energy (39-242KJ/mol) indicate rate control by the rate of attachment or detachment of ions at the andalusite-fluid interface. The effect of K-feldspar Al/Si disorder on the hydration rate was found to be consistent with the effect predicted by the change in the free energy of reaction. In mixed H_2O-CO_2 fluids, mullite was produced by the dehydration reaction rather than andalusite, which was produced by the reaction in pure H_2O. The rate of the dehydration reaction was found to be less in mixed H_2O-CO_2 fluids than in pure H_2O.

NOTATION

A_i	=	surface area of solid phase i
B_o	=	pre-exponential factor in Arrhenius equation
C_j	=	concentration of species j
D_j	=	diffusion coefficient of dissolved species j
D_j°	=	tracer diffusion coefficient of dissolved species j
E_D	=	activation energy of the dehydration reaction
f_{H_2O}	=	fugacity of H_2O
ΔG_f°	=	free energy of formation from the elements
ΔG_R	=	free energy change of reaction
ΔG_R°	=	standard state free energy change of reaction
J_j	=	flux of dissolved species j (moles cm^{-2} sec^{-1})
k	=	rate constant
k_D	=	rate constant, dehydration reaction

*Present Address: Battelle, Pacific Northwest Laboratories, P.O. Box 999, Richland, Washington 99352

**Present Address: Department of Geology and Geophysics, Yale University, New Haven, Connecticut 06520

k_H = rate constant, hydration reaction
n', n'' = exponents in rate law
n = constant
P = pressure
r = linear correlation coefficient
R = gas constant
R_D = rate of dehydration reaction
R_H = rate of hydration reaction
R_{net} = net rate of reaction
ΔS_R = entropy change of reaction
t = time
T = temperature
w_o = initial grain dimension of andalusite
V_{and} = volume of andalusite
X_{CO_2} = mole fraction CO_2 in fluid
$\eta^{\circ}_{H_2O}$ = viscosity of pure H_2O
ν = stoichiometric coefficient
ν_{ij} = moles of i per mole of j
σ_x = standard deviation of variable x

INTRODUCTION

Most previous experimental investigations of metamorphic reactions have considered systems at equilibrium. However, there is frequent evidence of disequilibrium in metamorphic rocks, for example, reaction rims on minerals, compositional zoning of minerals, and assemblages that are inconsistent with the phase rule. Study of the kinetics of metamorphic processes may shed light on these disequilibrium situations, provide information on metamorphic processes in general, and facilitate the interpretation of laboratory investigations. Reaction rate data may permit estimates of the time necessary for a disequilibrium assemblage to form, of heating and cooling rates, or of the duration of a tectonic episode. The study of reaction mechanisms, which is an integral part of the study of reaction kinetics, can yield important information on metamorphic processes, such as the role of the fluid phase, the effects of variations in mineral surface areas, the importance of nucleation versus growth of the product phases, and the relative ease of transport of various components.

Compared to studies of reaction equilibria, there have been relatively few experimental studies of metamorphic reaction kinetics. Fyfe, Turner and Verhoogen (1958) summarized much of the early work; Rubie and Thompson (1985) provide a more recent review. Some of the more recent studies include Greenwood's (1963) investigation of the rate of breakdown of talc to form enstatite + quartz and anthophyllite + quartz, as well as the rate of breakdown of anthophyllite to enstatite + quartz. Martin and Fyfe (1970) studied the rate of serpentinization of enstatite and forsterite. Wegner and Ernst (1983) investigated the reaction of forsterite with water to form serpentine, as well as the reverse dehydration reaction. Gordon (1971) investigated the rate of the reaction of calcite + quartz to form wollastonite in mixed H_2O-CO_2 fluids, Kridelbaugh (1973) investigated

the same reaction in pure CO_2, and Tanner, Kerrick, and Lasaga (1985) investigated this reaction in mixed H_2O-CO_2 fluids and in nearly pure CO_2. The rate of reaction of analcite + quartz to albite and the rate of formation of albite + quartz from jadeite were investigated by Matthews (1980).

This investigation is the study of the rates and mechanisms of the hydration-dehydration reactions:

$$\underset{(KAl_3Si_3O_{10}(OH)_2)}{\text{Muscovite}} + \underset{(SiO_2)}{\text{quartz}} \rightleftharpoons \underset{(Al_2SiO_5)}{\text{andalusite}} + \underset{(KAlSi_3O_8)}{\text{K-feldspar}} + \underset{(H_2O)}{\text{water.}} \quad (1)$$

These reactions were chosen for investigation for a number of reasons. Dehydration reactions are a common type of metamorphic reaction. The muscovite + quartz assemblage is common in metapelites, and the dehydration reaction is a reasonable analogue to an important metamorphic isograd reaction. The P-T equilibrium of reaction (1) is well established (Evans, 1965; Althaus and others, 1970; Storre and Karotke, 1971; Kerrick, 1972; Day, 1973; Chatterjee and Johannes, 1974). Reasonable agreement on the location of the equilibrium boundary exists between most of these studies.

An additional advantage of reaction (1) are the rates at which the hydration and dehydration reactions take place. Slow reaction rates at the pressure and temperature conditions of interest facilitate investigation using conventional cold-seal hydrothermal vessels, without the potential complications of reaction during the run-up or quench.

This study concentrates on the growth rates of the product phases in the presence of excess fluid. Nuclei for growth of the product phases were provided by using mixtures of the reactant and product phases as starting material. The role of nucleation in the hydration and dehydration reactions will be considered elsewhere (Schramke, Kerrick, and Lasaga, in preparation).

EXPERIMENTAL PROCEDURE

Starting materials.—Characterization of starting materials and sample preparation techniques are extremely important in the study of reaction kinetics. Variations in the crystallochemical properties of starting materials or in their preparation may influence the measured rates. All starting materials used in this study were natural mineral samples, with the compositions listed in table 1. Synthetic starting materials were not used because of potential problems with fine grain size and poor crystallinity.

The muscovite used in this study was from Methuen Township, Ontario, an occurrence originally described by Hurlbut (1956). This muscovite was obtained from the same locale as the material used in the Robie, Hemingway, and Wilson (1976) study of muscovite heat capacity. The muscovite was separated into thin sheets, and the edges were trimmed to remove potentially altered material. Any muscovite sheet with visible inclusions was discarded. The remaining material was ground in distilled water in a blender; this method of grinding should produce less damage to

the mineral structure than grinding with a mortar and pestle (G.W. Brindley, personal commun.). The muscovite was then X-rayed with a powder diffractometer using Cu Kα radiation, a Si standard, and a scanning rate of 1° 2θ per min. A unit cell refinement was carried out on the reflections using the program "UNIT CELL" (Appleman and Evans, 1973). The cell parameters obtained are consistent with the $2M_1$ muscovite polymorph.

Quartz for the experiments was taken from a large single crystal of Brazilian quartz. The quartz was powdered by crushing in a steel mortar and pestle. The quartz powder was then cleaned with a magnet and washed in cold, concentrated HCl to remove metal filings, followed by repeated washings in distilled water. In some experiments, quartz was in the form of single crystals, which had been ground into spheres which ranged in size from 0.1 to 0.2 cm in diameter.

The K-feldspar was adularia from Crystallina, Switzerland; the analysis in table 1 is from Kerrick (1972). In an attempt to minimize the complications that could arise from changes in Al/Si disorder during experimentation, the adularia was disordered to produce sanidine in the following manner. The feldspar was crushed, sieved, and heated at 1070°C in a 1 atm furnace for 21 days. The temperature and run length for the feldspar disordering were selected on the basis of Sipling and Yund's (1974) study of Al/Si disordering in alkali feldspars. The diffraction pattern of the feldspar before and after heating was obtained using a spinel standard (a = 8.0831 Å), Cu Kα radiation, and a scanning rate of 1° 2θ per min. The Al/Si disorder of the feldspar was calculated from the b and c cell parameters obtained from the unit cell refinements (Luth, 1974; Stewart

TABLE 1
Chemical composition of starting materials

	Muscovite*	Adularia**	Sanidine***	Andalusite****
SiO_2	45.11	64.39	62.71	32.27
Al_2O_3	34.14	18.58	17.9	60.99
FeO	2.27	0.03	0.02	0.24
MgO	0.27	0.00	—	0.00
CaO	0.00	0.00	0.00	0.02
Na_2O	0.73	1.14	1.03	0.05
K_2O	11.40	14.92	16.03	0.00
H_2O^+	4.13	0.08	—	—
H_2O^-	—	0.00	—	—
TiO_2	0.31	0.00	0.08	0.04
P_2O_5	—	0.00	—	—
MnO	0.01	0.00	0.01	0.02
F	0.30	0.00	—	—
SrO	—	0.035	—	—
BaO	—	0.82	0.72	0.00
Rb_2O	—	0.03	—	—
Total	98.67	100.03	98.50	99.63

*Microprobe analysis, average of seven analyses. F analysis by J. Bodkin. H_2O^+ analysis by author.
**From Kerrick (1972), C. O. Ingamells, analyst.
***Microprobe analysis, average of seven analyses.
****Microprobe analysis, average of three analyses.

and Wright, 1974), and the feldspar was found to be completely disordered. The feldspar was then ground to a finer grain size in an agate mortar and pestle.

The andalusite used in these experiments consisted of gem-quality crystals from Minas Gerais, Brazil. The crystals were pale pink and transparent, with an occasional pale green crystal. The composition of a pink andalusite crystal was checked on the electron microprobe (table 1). The Fe content of the mineral, calculated as FeO, ranged from 0.20 to 0.27 wt percent. Holdaway (1971) found that the only compositional variations between pink and green andalusite crystals from this locality were small variations in the Fe_2O_3 and MnO contents. The andalusite crystals were crushed in a steel mortar and pestle and treated to remove metal filings in the same manner as the quartz powder.

Sillimanite is the aluminum-silicate polymorph most commonly produced by the dehydration reaction in metamorphic rocks. Andalusite was used instead of sillimanite for a number of reasons. Gem-quality andalusite samples are easily obtained, whereas many sillimanite specimens contain fibrolite, which is typically fine-grained and often intergrown with other phases. In addition, melting occurred in the experiments with mixtures of all four solid starting materials plus excess water that were conducted in the sillimanite stability field. Most experiments were therefore conducted in the andalusite stability field (Holdaway, 1971), and the most stable polymorph was used.

All four mineral powders were sieved to between 325 and 400 mesh (sieve openings of 45 and 38 microns, respectively). The muscovite was sized by washing through stainless steel sieves with distilled water; the other minerals were sieved dry. The minerals were then treated in the following manner to remove micron-sized particles from the surfaces. Each mineral was washed ultrasonically in acetone, and the supernatant liquid was decanted. This process was repeated five times using acetone, then three times using distilled water, until the supernatant liquid was clear and free of suspended particles. The andalusite, K-feldspar, and quartz were then etched for 20 min in a solution of 0.09 N H_2SO_4 and 5 percent HF, to remove surface material damaged during the grinding process. The acid solution was identical in composition to the solution used by Holdren and Berner (1979). The minerals were subsequently rinsed in distilled water, and the complete ultrasonic cleaning process was repeated. The muscovite was not etched in the H_2SO_4-HF solution because of possible fluorine-hydroxyl exchange between the mica and solution. After the etching and ultrasonic treatments, SEM examination of the solid starting materials (pls. 1-4) revealed that the mineral surfaces were virtually free of adhering particulate matter.

Experiments for the hydration reaction were conducted with powdered mixtures of all four solid starting materials, using equal weights of each phase. For experiments involving the dehydration reaction, mixtures consisted of equal weights of muscovite, sanidine, and andalusite, and quartz provided by single crystals. The quartz single crystal technique was used only to monitor the dehydration reaction,

PLATE 1

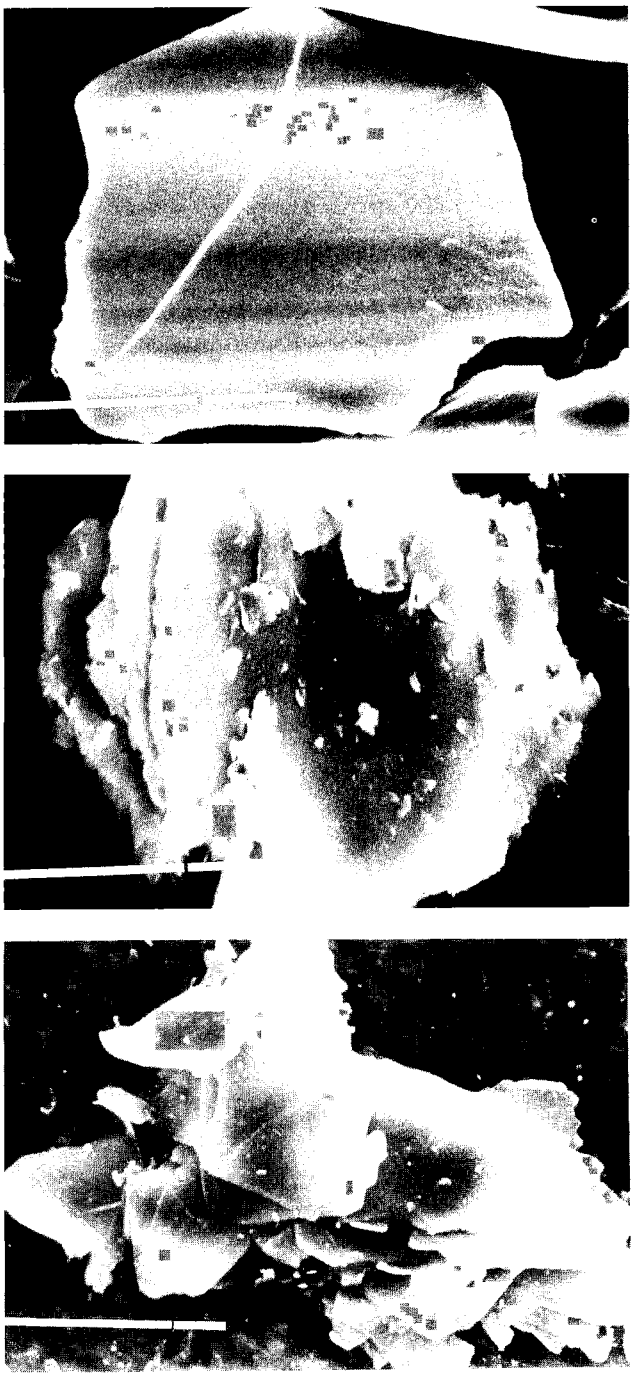

A.

B.

C.

PLATE 2

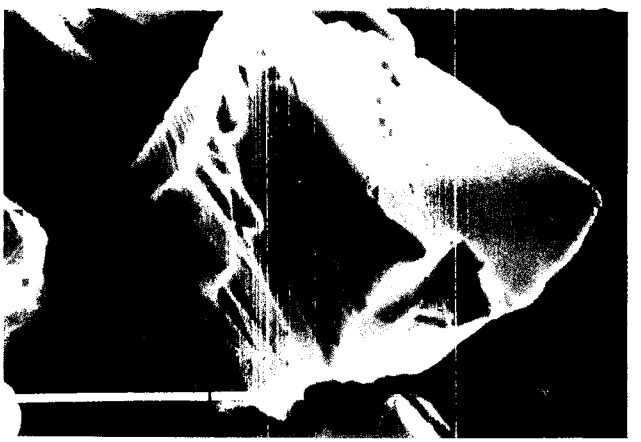

A.

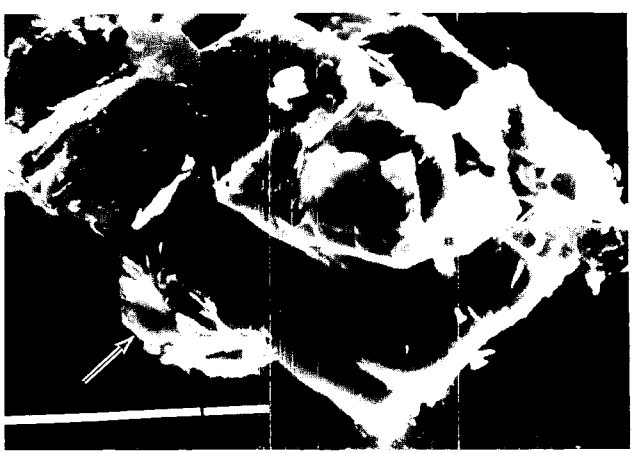

B.

SEM photographs of crushed quartz grains. The short white scale bar in each photograph is 5 microns in length: (A) starting material, washed and etched in acid solution to remove adhering particles produced by grinding, (B) after hydration reaction at 500°C and 3 kb for 1.4 days. The arrow in the photograph points out an adhering clump of muscovite.

← SEM photographs of muscovite grains. The short white scale bar in each photograph is 5 microns in length: (A) starting material, washed to remove adhering particles produced by grinding, (B) after hydration reaction at 500°C and 3 kb for 1.4 days, (C) after dehydration reaction at 700°C and 1 kb for 1.5 days.

PLATE 3

because nucleation and growth of quartz in the powder as well as on the single crystal (Hunt and Kerrick, 1977) during the hydration reaction could yield anomalously low values for the amount of reaction. After the powdered components of the mixtures were weighed, they were stirred thoroughly, dried for 24 hrs at 220°C in air to remove adsorbed water, and stored in a desiccator. Homogeneity of the mixtures was checked by decomposing nine weighed samples of the mixtures at 700°C in a 1 atm furnace. The weight loss of the samples caused by the heat treatment corresponded, within the limits of weighing error ($\pm 2 \times 10^{-5}$ g), with the weight loss expected from dehydration of the amount of muscovite in a homogeneous mixture.

Run procedure.—Reaction mixtures consisting of 0.030 g of powder were loaded into Ag_{50}-Pd_{50} capsules. In the dehydration reaction experiments, half the powder was loaded into the capsule, the quartz crystal was added, and the remaining powder was packed on top. About 0.0075 g of distilled H_2O were added to the weighed capsule, the capsule was weighed again to determine the precise amount of H_2O, then welded shut. Thus, a known weight of H_2O was present in the capsule at the beginning of the experiment, and a volume equal to a minimum of 85 percent of the solids volume was occupied by water at the experimental conditions. Variation of the weight of water in the capsules by a factor of two in either direction did not affect the results of the experiments. In a few experiments, mixed H_2O-CO_2 fluids were used. In these experiments, CO_2 was generated by placing a weighed amount of silver oxalate in the capsules. The capsules used in the mixed-volatile experiments were otherwise identical to those containing pure H_2O.

Three identical capsules were used in each experiment to permit an estimation of analytical error. The capsules were placed in cold-seal hydrothermal pressure vessels, which were horizontally mounted in split furnaces. Chromel-alumel thermocouples were placed in external thermocouple wells, and filler rods were used in all runs to minimize temperature gradients. All thermocouples were checked at regular intervals against reference thermocouples constructed from chromel and alumel wires calibrated by the National Bureau of Standards. The combined temperature uncertainty caused by controller drift and thermocouple error is estimated to be ±5°C. Pressure was monitored continuously during the run with a Bourdon-tube gauge. These gauges were checked periodically against a standard gauge, which had been calibrated with a dead-weight gauge. The pressure uncertainty caused by temperature fluctuation and gauge error is estimated to be ±50 bars.

← SEM photographs of andalusite grains. The short white scale bar in each photograph is 5 microns in length: (A) starting material washed and etched in acid solution to remove adhering particles produced by grinding, (B) after hydration reaction at 500°C and 3 kb for 1.9 days. The arrows in the photograph indicate rectangular etch pits, (C) after dehydration reaction at 700°C and 1 kb for 1.5 days. The arrow in the upper left of the photograph indicates a step-growth feature.

PLATE 4

A.

B.

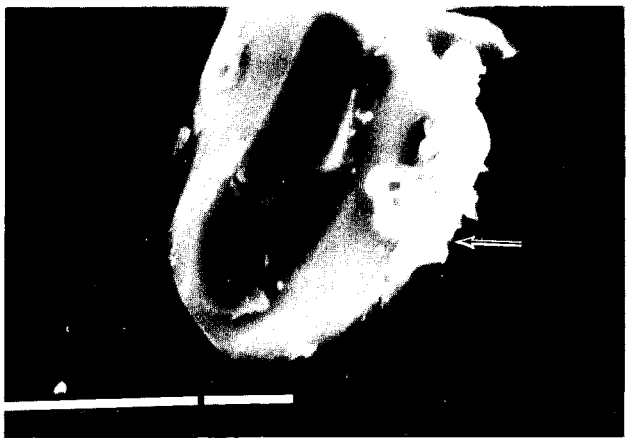

C.

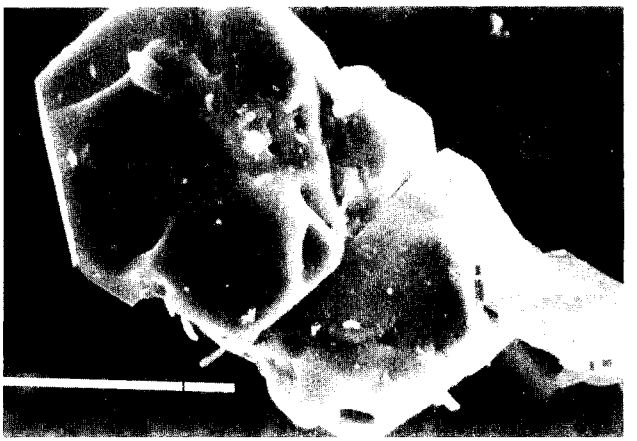

The experiments were carried out in the following manner. For experiments conducted at pressures up to and including 2 kb, the system was initially pressurized to 1 kb; experiments conducted at pressures greater than 2 kb were initially pressurized to 1.5 kb less than the run pressure. The vessel was heated, and the pressure was allowed to increase. Typically, the system reached the P-T conditions of the run within 20 to 30 min. The beginning of each experiment (time = 0) was taken at the time when the system was within 10°C of the run temperature. At the end of an experiment, the vessel was removed from the furnace and placed in a stream of compressed air. The temperature typically dropped to less than 200°C in 2 min or less.

The pressurization step prior to heating could have crushed the starting materials, resulting in increased mineral surface areas. Therefore, capsules filled with the starting materials were pressurized without heating to 3½ kb, the maximum pressure before heating, and the contents were examined for evidence of crushing. The capsules were impregnated with epoxy resin, thin-sectioned, and examined with a petrographic microscope. No evidence of crushing was observed. In addition, oil immersion mounts of the material from these capsules, examined with an optical microscope, indicated that little or no crushing of the starting materials occurred.

The possibility that measurable reaction occurred during the run-up or quench was checked by taking a number of capsules to pressures and temperatures within the range of this study, then quenching the experiments as soon as they had reached the experimental conditions. Analysis of the capsules in these experiments confirmed that at time = 0, no detectable reaction had taken place. Essentially all reaction therefore took place at isothermal, isobaric conditions.

After completion of an experiment, the capsules were centrifuged to force the water to one end, weighed, and punctured. If CO_2 was used in the experiment, the weight loss after puncture corresponded to the weight of CO_2 present in the capsule. The capsules were then dried overnight at 110°C, after which they were weighed again. The weight loss after drying corresponded to the weight of H_2O present at the end of the run. Because the initial weight of H_2O was known, the change in weight of H_2O could be calculated, and the amount of reaction that took place was thus determined. The accuracy and precision of this technique was tested with capsules loaded with water alone. The error was found to be $\pm 2 \times 10^{-5}$ g, or about 1×10^{-6} moles of H_2O. If a quartz single crystal was used in the experiment, it was removed from the capsule following analysis of the change in weight of H_2O and cleaned ultrasonically in acetone and in

← SEM photographs of sanidine grains: The short white scale bar in each photograph is 5 microns in length: (A) starting material, washed and etched in acid solution to remove adhering particles produced by grinding, (B) after hydration reaction at 500°C and 3 kb for 1.4 days. The arrow indicates an adhering clump of muscovite, (C) after dehydration reaction at 675°C and 2 kb for 5 days.

TABLE 2
Results of quartz solubility experiments

P(kb)	T°C	Δweight quartz (grams)	molal solubility (experiments)	calculated molal solubility (Fournier and Potter, 1982)
1	500	1.6×10^{-5}	0.036 ± 0.022	0.042
1	600	2.6×10^{-5}	0.058	0.047
1	700	2.5×10^{-5}	0.055	0.056
2	600	5.0×10^{-5}	0.111	0.112
2	650	6.0×10^{-5}	0.133	0.135
2	675	6.4×10^{-5}	0.142	0.149

distilled water. The weight of a crystal before and after experimentation was determined by five replicate weighings on a microbalance.

The weight change of each quartz crystal was corrected to allow for dissolution of quartz in the aqueous fluid by conducting a separate series of experiments at the same pressures and temperatures as the experiments for the investigation of reaction(1). The solubility experiments contained a weighed single crystal of quartz, 0.0075 g of sanidine, and 0.0075 g of water. The presence of sanidine in the capsule presumably mimicked the common ion effect of the silicates in reaction (1). Because the assemblage sanidine + quartz + water is stable throughout the experimental P-T range, the weight loss of the quartz crystal should be due solely to equilibration of the quartz crystal with the solution. The minimum length of the experiments was four days. At the end of an experiment, the quartz crystals were removed from the capsules, and the weight loss and solubility of quartz in the aqueous fluid were determined. These data, listed in table 2, were used to correct for the effects of equilibration of the quartz with the solution in the experiments on reaction (1). The solubility of quartz in the fluid was identical, within the limits of experimental error, to the solubility of quartz in a pure aqueous fluid (table 2) calculated using the equation of Fournier and Potter (1982). The effect of the presence of other silicates on the quartz solubility in the fluid therefore appears to be minimal. The correction of the quartz weight loss due to solubility does not affect the reaction rate: rather, it merely affects the comparison of the change in moles of H_2O and quartz in the experiments. Within an experiment, the variation in the change in weight of the three quartz spheres was generally within a 2×10^{-5} g range. Similar variation was found when monitoring the change in weight of H_2O, but because of the higher gram molecular weight of quartz, the precision of the quartz single crystal technique, on a molar basis, was better than for H_2O alone.

EXPERIMENTAL RESULTS AND DISCUSSION

Effects of preparation of starting materials.—Hydration and dehydration experiments were conducted at 2 kb, at 450°C and 675°C to determine the effects of the ultrasonic cleaning and etching of the starting materials on the experimental results. For the hydration and dehydration reactions, a series of experiments was conducted with mixtures of starting materials that had not been etched and cleaned, as well as with mixtures composed of starting materials that had been etched and ultrasonically

cleaned as described in the previous section. For the hydration reaction (fig. 1A), the amount of reaction observed when untreated starting materials were used was consistently higher than the amount observed when etched and ultrasonically cleaned starting materials were utilized. For example, at time = 4 days, 1.5×10^{-5} moles of water were consumed by the reaction of the untreated materials, whereas using the etched and cleaned materials, less than 1.1×10^{-5} moles of water were consumed. The shapes of the curves in plots of the amount of reaction as a function of time for the treated and untreated materials were not significantly different, in contrast with the results of Holdren and Berner (1979) in their study of feldspar dissolution.

For the dehydration experiments at 675°C and 2 kb, relatively small differences exist between the results obtained with the two sets of starting materials (fig. 1B). The etched and cleaned starting materials appear to have reacted slightly less than the untreated material, but this difference may not be statistically significant. Because of the demonstrated effect of the etching and cleaning steps on the experimental results of the hydration reaction, for the remainder of this study, the starting materials were etched and ultrasonically cleaned as outlined in the previous section.

Etching with the $HF-H_2SO_4$ solution may have altered the surface composition of the starting materials. Perry, Tsao, and Gangler (1983) found that after treatment of K-feldspar with this solution, fluorine and sulfur were present on the surface. Based on their data, only a very thin layer of the etched starting materials should have been altered. Consequently, it was assumed that the effects of such a layer on the reaction rates were minor because of the small volume of material affected by this pretreatment. In comparison, Holdren and Berner (1979) demonstrated that the effects of the surface material damaged by grinding can be significant. Therefore, etching of the starting materials was necessary.

Reaction rates.—A series of four-day experiments were carried out over a temperature range of 350° to 700°C at pressures that ranged from 0.5 to 5 kb to determine the general dependence of the reaction rate as a function of temperature and pressure. The fraction of reaction that took place was obtained by dividing the change in moles of quartz or H_2O by the number of moles of the least abundant (on a molar basis) reactant phase in the capsule. In the dehydration and hydration experiments, the least abundant reactant phases were muscovite and sanidine, respectively. Contours of the fraction of reaction on both sides of the equilibrium boundary appear in figure 2. The area above the contour labelled "1.00" is the region where the hydration reaction went to completion in four days or less.

The quantity measured in these experiments is proportional to R_{net}, the net rate of reaction. From transition state theory applied to overall reactions, R_{net} may be expressed as a function of temperature and the free energy change of the dehydration reaction, ΔG_R (Fisher and Lasaga, 1981):

$$R_{net} = B_o e^{-E_D/RT} (1 - e^{n\Delta G_R/RT}), \qquad (2)$$

if an Arrhenius temperature dependence is assumed for the dehydration

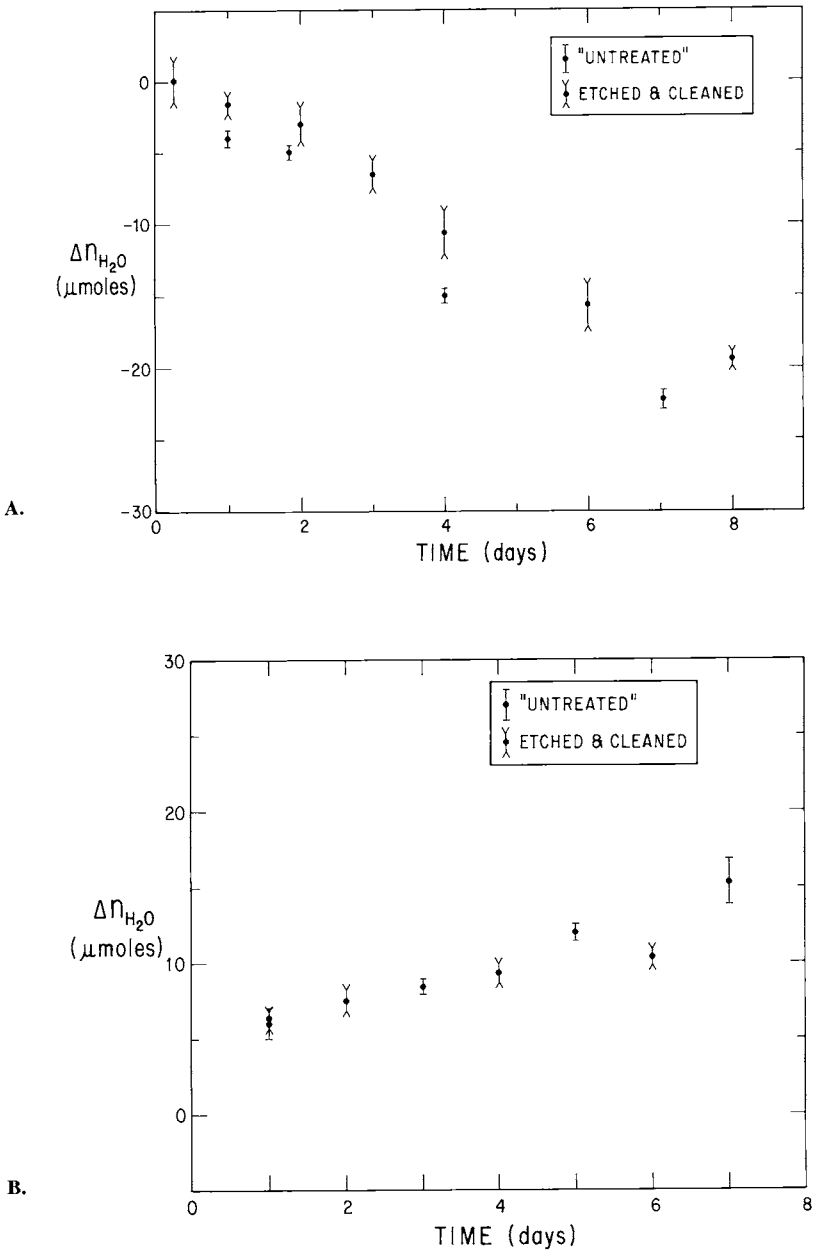

Fig. 1. Comparison of results of experiments carried out on mixtures of starting materials that were etched and washed to remove damaged surface material and mixtures that were not treated after grinding: (A) 450°C, 2 kb hydration reaction, (B) 675°C, 2 kb dehydration reaction.

reaction rate. In eq (2), B_o is the pre-exponential factor, E_D is the apparent activation energy of the dehydration reaction, and n is a constant.

This equation may be used to explain qualitatively the variation in the mole fraction of reaction (and hence, R_{net}) as a function of temperature and pressure. On the dehydration side of the equilibrium boundary, increasing the distance from the equilibrium boundary increases the magnitude of ΔG_R and hence increases the net rate of reaction.

On the hydration side of the equilibrium boundary, the reaction rate as a function of temperature is determined by the competing effects of the two exponential terms in eq (2). An isobaric decrease of temperature from a point on the equilibrium boundary should at first increase the net reaction rate because of the increase in ΔG_R. As temperature declines further, the reaction rate reaches a maximum and then decreases as the effect of the first exponential term overwhelms the effect of increasing ΔG_R. For reaction (1), these competing factors produced a rate maximum

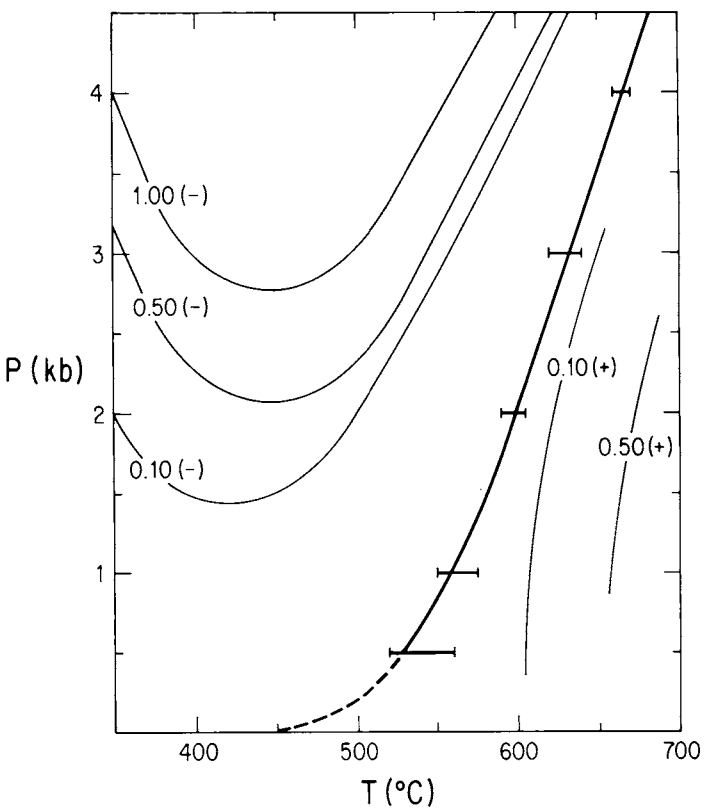

Fig. 2. Contoured diagram of the fraction of reaction after 4 days for the hydration (-) and dehydration (+) reactions as functions of temperature and pressure. The equilibrium boundary and brackets are from Chatterjee and Johannes (1974).

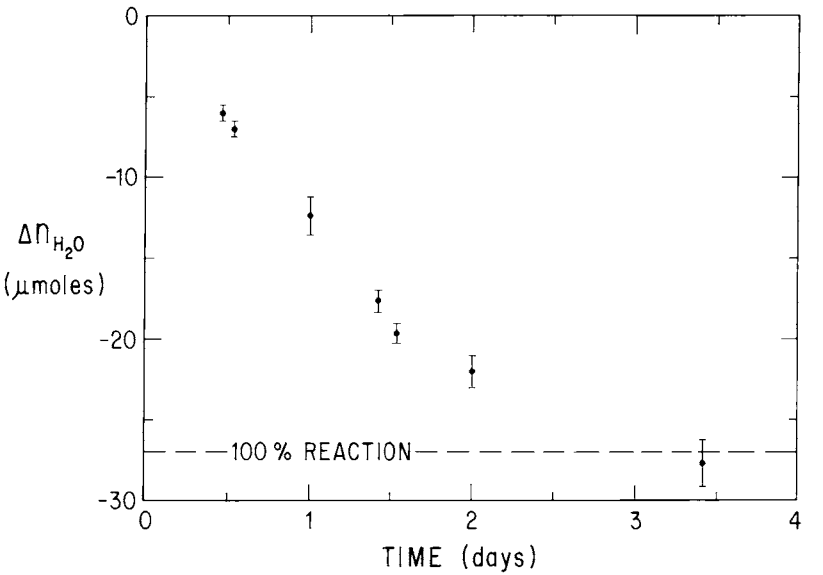

Fig. 3. Example of the results of the isothermal, isobaric hydration experiments: 500°C, 3 kb.

centered at approx 450°C. If pressure is isothermally raised on the hydration side of the equilibrium boundary, ΔG_R is increased, and the net rate is thus increased.

Additional experiments were conducted over a range of pressure and temperature conditions to determine reaction rates. Time versus extent of reaction experiments were carried out at 400°, 450°, and 500°C at 2 kb, and at 500°C at 3 kb to investigate the rates of the hydration reaction. As an example, results of the 500°C, 3-kb experiments are plotted in figure 3. The complete data set is described in detail in Schramke (ms). The hydration reaction data indicate an initial linear dependence of the extent of reaction on time and an intercept of approximately zero within $\pm 2\sigma$. An abrupt decrease in the reaction rate occurred as the extent of reaction approached 100 percent. The reaction rate dropped off sharply as the feldspar present in the capsule was consumed. The slope of the linear region is equal to the initial reaction rate (dn_{H_2O}/dt). Reaction rates were obtained using the weighted least-squares linear regression program LINFIT (Bevington, 1969). The reaction rates obtained from the best-fit lines are listed in table 3.

Detailed rate studies of the dehydration reaction were conducted at 600°, 650°, and 700°C at 1 kb, and 600°, 650°, and 675°C at 2 kb. As an example, results of the 1 kb, 650°C experiments are illustrated in figure 4. The complete data set is described in detail elsewhere (Schramke, ms). The data in figure 4 describe a parabolic curve. The rapid initial reaction rate is believed to result from reaction of muscovite that was damaged during grinding. This damaged material was probably not removed during

sample preparation because the muscovite was not acid etched. To determine if the reaction of damaged muscovite caused the rapid initial reaction in the hydration experiments, a number of capsules containing a quartz single crystal and a mixture of equal weights of the other powdered starting materials were run at 650°C and 1 kb for 3 days. If damaged muscovite was the cause of the rapid initial reaction rate, then a second set of experiments conducted with the mixture run in these 3-day experiments should not display the rapid initial rate (that is, the first experiments should have removed most of the damaged material). The material was removed from the capsules, reloaded into new capsules, and a series of experiments was conducted at 1 kb and 650°C using this "annealed" material. The results of experiments with the initial and "annealed" starting materials appear in figure 5. Because of scatter in the data obtained from the "annealed" material, it is difficult to draw a conclusion from these experiments. However, the intercept of the best-fit line to the "annealed" material data is somewhat smaller than that of the initial material and is zero within $\pm 2\sigma$ about the line. Therefore, the rapid reaction rate during the early stages of the dehydration experiments may have been caused by reaction of damaged muscovite; consequently, the rates of the dehydration reaction were determined from the slope of the line fit to the data excluding the region of rapid initial reaction. For example, in figure 4 there is an apparent change in slope at 3 days reaction time, so the 1- and 2-day data points were excluded. The fit to the data was obtained in the same manner as in the hydration experiments.

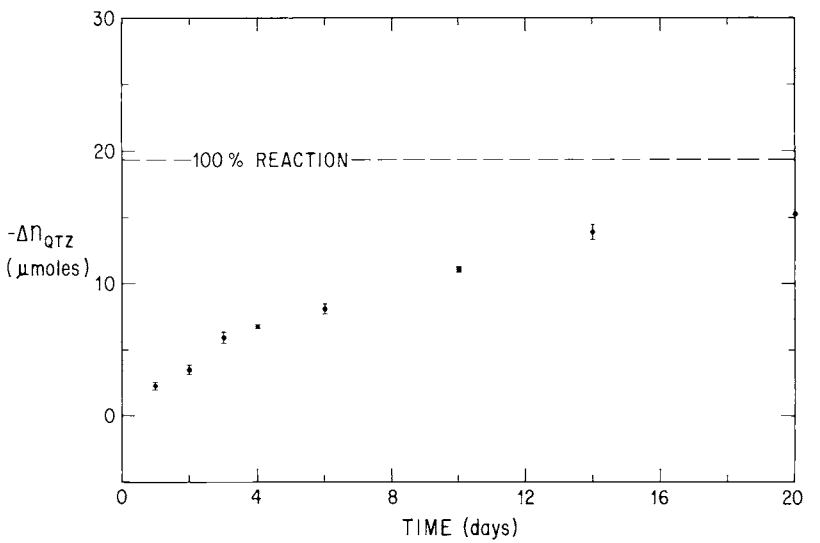

Fig. 4. Example of the results of the isothermal, isobaric dehydration experiments: 650°C, 1 kb.

TABLE 3
Measured reaction rates, values in parentheses are one standard deviation (σ)

Hydration reaction: Muscovite + Quartz ← Andalusite + Sanidine + H_2O

P(kb)	T°C	Weight proportions in mix	rate (μmoles/hr)	intercept (μmoles)	r	data points
2	350	equal weights	-0.02100(0.01425)	-9.3750(2.9681)	0.981	3
2	400	(B) equal weights*	-0.14688(0.01115)	1.9070(1.1989)	0.999	5
		(A) equal weights*	-0.08180(0.005777)	0.57089(0.77319)	0.986	5
		2x muscovite	-0.15229(0.01507)	0.20303(0.82334)	0.999	4
		2x quartz	-0.16665(0.01770)	0.49901(1.26344)	0.994	4
		2x sanidine	-0.17852(0.00916)	2.3095(0.71130)	0.988	5
		2x andalusite	-0.24564(0.01388)	-3.2330(2.1235)	0.992	4
2	450	(B) equal weights*	-0.18026(0.01585)	1.7032(1.2062)	0.993	4
		(A) equal weights*	-0.10633(0.00446)	0.92932(0.54016)	0.998	7
		2x muscovite	-0.20834(0.01273)	0.20913(0.7665)	0.959	5
		2x quartz	-0.145533(0.03216)	-1.7129(2.4817)	0.991	4
		2x sanidine	-0.14279(0.01414)	0.41613(0.84246)	0.996	4
		2x andalusite	-0.25026(0.01404)	2.5949(1.1604)	0.998	5
2	500	equal weights	-0.03649(0.00330)	0.59544(0.73220)	0.977	4
3	500	equal weights	-0.51884(0.02441)	-0.23870(0.64408)	0.998	5
		2x muscovite	-0.52250(0.03354)	-1.9938(0.83327)	0.995	4
		2x quartz	-0.62075(0.05860)	2.4307(1.1404)	0.978	5
		2x sanidine	-0.56607(0.05572)	-0.00093(1.4171)	0.982	5
		2x andalusite	-0.81358(0.06574)	2.1556(1.6100)	0.995	4

Dehydration reaction: Muscovite + Quartz → Andalusite + Sanidine + H_2O

P(kb)	T°C	Weight proportions in mix	rate (μmoles/hr)	intercept (μmoles)	r	data points
1	600	equal weights	0.010245(0.00060)	0.43300(0.06316)	1.000	3
1	650	equal weights	0.03037(0.00085)	3.7844(0.1827)	1.000	5
		2x muscovite	0.05035(0.00183)	2.5708(0.2381)	0.988	8
		2x sanidine	0.02095(0.00515)	7.3740(1.1872)	0.982	4
		2x andalusite	0.05692(0.00167)	4.5417(0.2116)	0.987	5
1	700	equal weights	0.17332(0.00845)	2.9632(0.17882)	0.991	4
		2x muscovite	0.15878(0.00663)	5.2658(0.24902)	0.839	7
		2x sanidine	0.19724(0.00246)	3.7246(0.10422)	0.998	7
		2x andalusite	0.27592(0.00596)	4.3987(0.12937)	0.994	5
2	600	equal weights	-0.00052(0.00084)	0.33750(0.05328)	0.497	3
2	650	equal weights	0.014716(0.00156)	2.8704(0.12705)	0.959	4
2	675	equal weights	0.06011(0.00364)	4.2058(0.24498)	0.900	5
		2x muscovite	0.06307(0.00388)	5.0280(0.43131)	0.987	4
		2x sanidine	0.06031(0.00262)	3.5279(0.27370)	0.908	4
		2x andalusite	0.15939(0.00347)	2.0400(0.16821)	0.849	4

Dehydration reaction: $X_{CO_2} = 0.48$, Muscovite + Quartz → Andalusite + Sanidine + H_2O

P(kb)	T°C	Weight proportions in mix	rate (μmoles/hr)	intercept (μmoles)	r	data points
1	700	equal weights	0.05675(0.0099)	5.966(1.158)	0.992	3

Hydration reaction: Muscovite + Quartz ← Andalusite + Adularia + H_2O

P(kb)	T°C	Weight proportions in mix	rate (μmoles/hr)	intercept (μmoles)	r	data points
2	450	equal weights	-0.065703(0.009072)	1.2307(0.8224)	0.985	3

*See text.

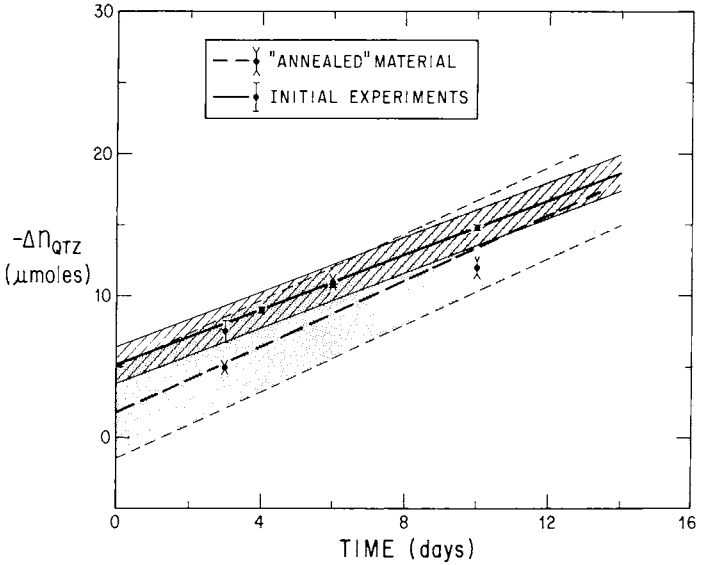

Fig. 5. Comparison of the results of the dehydration experiments conducted at 650°C and 1 kb with hydrothermally "annealed" material and with material prepared without annealing.

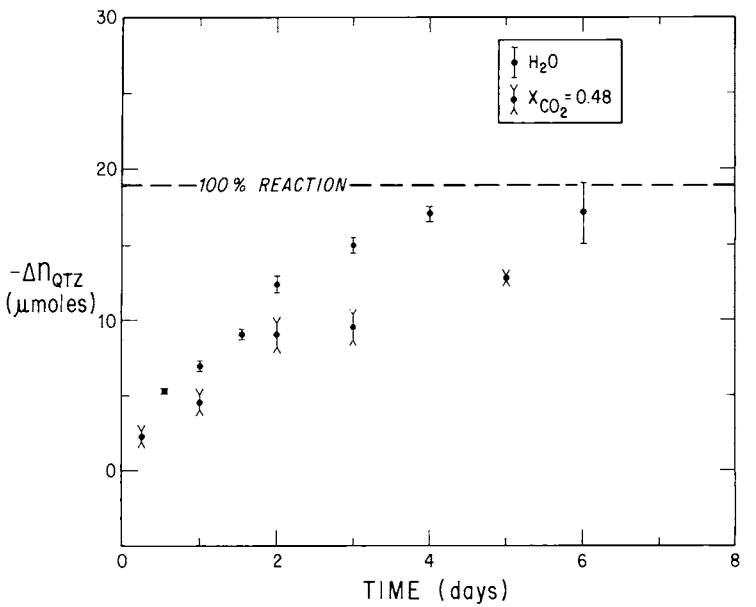

Fig. 6. Results of dehydration experiments at 700°C and 1 kb, in a fluid with X_{CO_2}=0.48 and in a pure aqueous fluid.

A series of experiments were conducted at 1 kb and 700°C, in the presence of a mixed H_2O-CO_2 fluid of final composition $X_{CO_2} = 0.48$. Because of the small amount of H_2O produced by reaction (1), compared to the amount of fluid present in the capsules, the initial and final values of X_{CO_2} were virtually identical. The reaction rate was monitored by the change in weight of quartz single crystals, and, except for the composition of the fluid phase, the experiments were identical to the dehydration experiments conducted with pure water. The results of the mixed-volatile experiments are compared to the data for pure water in figure 6.

Stoichiometry of the reaction.—It is important to ascertain that the reaction being studied actually proceeded as written. The dehydration reaction was monitored by both the number of moles of H_2O evolved and the moles of quartz consumed. Assuming that the correction for quartz solubility was accurate (table 2), the absolute value of the change in moles of quartz should equal the change in moles of H_2O. The change in moles of quartz was compared to the change in moles of H_2O in all dehydration experiments and was found to be equal within the limits of measurement. The respective slopes obtained by fitting lines to the change in moles of water and of quartz as functions of time agreed within $\pm 2\sigma$ for all dehydration experiments conducted in this study. In each case, the width of the 2σ band about the quartz data was narrower than the band about the H_2O data. The more precise quartz data were therefore used to determine reaction rates for the dehydration reaction.

Run products from experiments at various P-T conditions were checked by obtaining a powder X-ray diffraction pattern of the run products from the experiments of the longest duration. The X-ray diffractometer used should have detected any phases present in amounts greater than 5 wt percent of the mixture. The only phases detected were those involved in reaction (1) as written. On the hydration side of the equilibrium boundary, the reaction:

$$\underset{(Al_2Si_4O_{10}(OH)_2)}{\text{Pyrophyllite}} \rightleftarrows \underset{(Al_2SiO_5)}{\text{andalusite}} + 3\ \underset{(SiO_2)}{\text{quartz}} + \underset{(H_2O)}{\text{water}}. \qquad (3)$$

may stably produce pyrophyllite at 350°C and 2 kb. All other hydration experiments took place within the stability field of andalusite + quartz (Kerrick, 1968; Haas and Holdaway, 1973). No pyrophyllite was detected in diffraction patterns of the run products. Assuming a maximum of 5 wt percent pyrophyllite, the maximum undetected error reaction (3) could have introduced is approx 4×10^{-6} moles of water.

On the dehydration side of the equilibrium boundary, corundum + quartz could have been produced instead of andalusite. Day (1973) found that an experiment at 650°C, 2 kb with starting materials of muscovite + quartz produced a mixture of sanidine, corundum, and quartz. The production of corundum + quartz is unlikely, however, in experiments that include andalusite in the starting mixtures, because andalusite is more stable at the experimental conditions. Furthermore, X-ray diffraction, SEM, and petrographic examination of run products revealed no corundum. The good correlation between the change in moles of quartz

and the change in moles of H_2O in dehydration reaction experiments is further indication that significant production of corundum + quartz did not occur.

Another possible problem was nucleation and growth of aluminum-silicate polymorphs other than andalusite (for example, mullite or sillimanite). SEM, petrographic, and X-ray diffraction examination of the run products indicated that the aluminum-silicate produced by the dehydration reaction was andalusite. One experiment, at 700°C, 1 kb and of 4 days duration, contained a small amount of a phase identified as mullite in the X-ray diffraction pattern. This experiment was the only dehydration experiment that appeared to have any aluminum-silicate other than andalusite. This experiment, in which nearly 100 percent reaction had taken place, was not used in the determination of the reaction rate.

In X-ray diffraction patterns of the run products, the peaks of the product phases were qualitatively observed to increase with a corresponding decrease in the height of the peaks of the reactant phases. No attempt was made to quantify this observation. K-feldspar diffraction peaks obtained from run products of experiments at 650° and 1 kb, 700°C and 1 kb, and at 675°C and 2 kb were indexed, and a cell refinement was carried out using the reflections obtained. The feldspar unit cell parameters did not change relative to the parameters of feldspar in the starting materials. The basal peak of muscovite in diffraction patterns of run products from the hydration experiments was somewhat broadened relative to the muscovite starting material. There were insufficient muscovite peaks present to permit a unit cell refinement of the muscovite in the run products. It was difficult to identify the muscovite polytype(s) present in the run products because of interference by other phases that were present. Amouric and Baronnet (1983) found that synthetic muscovite nucleated and grown at 500°C, 1 kb consisted of a mixture of 1M and $2M_1$ muscovite polytypes. If 1M muscovite was produced by reaction (1), it was probably a reaction intermediary. The stable muscovite at these P-T conditions is the $2M_1$ polytype, and with sufficient time at the run conditions, 1M muscovite should convert to $2M_1$.

The hydrolysis reactions:

$$\underset{(KAlSi_3O_8)}{3\text{ sanidine}} + \underset{(H_2O)}{2\text{ water}} \rightleftarrows \underset{(KAl_3Si_3O_{10}(OH)_2)}{\text{muscovite}} + \underset{(SiO_2)}{6\text{ quartz}} + 2\ KOH_{(aq)} \quad (4)$$

$$\underset{(KAlSi_3O_8)}{2\text{ sanidine}} + \underset{(H_2O)}{\text{water}} \rightleftarrows \underset{(Al_2SiO_5)}{\text{andalusite}} + \underset{(SiO_2)}{5\text{ quartz}} + 2\ KOH_{(aq)} \quad (5)$$

$$\underset{(KAl_3Si_3O_{10}(OH)_2)}{2\text{ muscovite}} \rightleftarrows \underset{(Al_2SiO_5)}{3\text{ andalusite}} + \underset{(SiO_2)}{3\text{ quartz}} + 2\ KOH_{(aq)} + \underset{(H_2O)}{\text{water}} \quad (6)$$

can be written for the phases present in the experiments of this study. Although any two of reactions (4) to (6), when added together, yield the overall reaction (1), these hydrolysis reactions are not proposed as steps in the reaction mechanism. If any one of these reactions took place to a measurable extent independently of overall reaction (1), the balance of the

change in moles of water and quartz would have been disturbed. Such an imbalance was not observed in the dehydration experiments. As a further check, an empirical study was carried out in which capsules containing the solid reactants and products of the individual hydrolysis reactions plus excess H_2O were run at P-T conditions representative of the hydration and dehydration experiments. The only reaction that appeared to take place to a measurable extent was the overall hydration or dehydration reaction (1). These results are consistent with a similar empirical investigation by Kerrick (1972).

Reaction mechanism.—Run products from the hydration and dehydration experiments were examined with an SEM. Such an examination may provide information on the sites at which growth of product phases occurred. In addition, further information may be obtained from textural features of the run products.

SEM examination of the run products of the hydration experiments revealed that small flakes of muscovite grew on the muscovite starting material (pl. 1-B), and precipitation of quartz took place on preexisting grains (pl. 2-B). The surfaces of the muscovite and quartz grains were checked qualitatively with the energy-dispersive system (EDS) on the SEM, and the compositions of the overgrowths on the grains were consistent with the compositions of the starting materials.

Andalusite (pl. 3-B) had an angular appearance, with some pitting of the surface. In comparison, sanidine had a rounded appearance (pl. 4-B). Andalusite and sanidine grains were checked qualitatively with EDS, and there was no evidence of incongruent dissolution. The andalusite, sanidine, and quartz grains had adhering flakes of muscovite, but the surfaces of the minerals were not covered by muscovite, and there was no evidence of "armoring" of reactant grains by product phases. The flakes of muscovite may have nucleated and grown on the surfaces of the other minerals or may have been detached from muscovite aggregates during removal from the capsule. It is not known how firmly the muscovite was attached to the andalusite and sanidine surfaces.

Andalusite grains from the dehydration experiments (pl. 3-C) had jagged, angular overgrowths, with some evidence of step-growth features. In comparison, sanidine grains from the dehydration experiments had much smoother, more regular surfaces (pl. 4-C). The composition of the andalusite and sanidine overgrowths were checked qualitatively with EDS. Growth of the product phases appears to have taken place on preexisting product grains. Plates 1-C and 5-B illustrate the typical appearance of muscovite and quartz in run products of the dehydration reaction.

The mechanisms by which the hydration and dehydration reactions took place may be outlined as follows. Both reactions occurred through dissolution of reactant phases, transport of dissolved material through the fluid phase, and precipitation onto preexisting product grains. The mechanism of the hydration and dehydration reactions is therefore a set of two dissolution and two precipitation processes, linked by the stoichiometry of the overall reaction.

PLATE 5

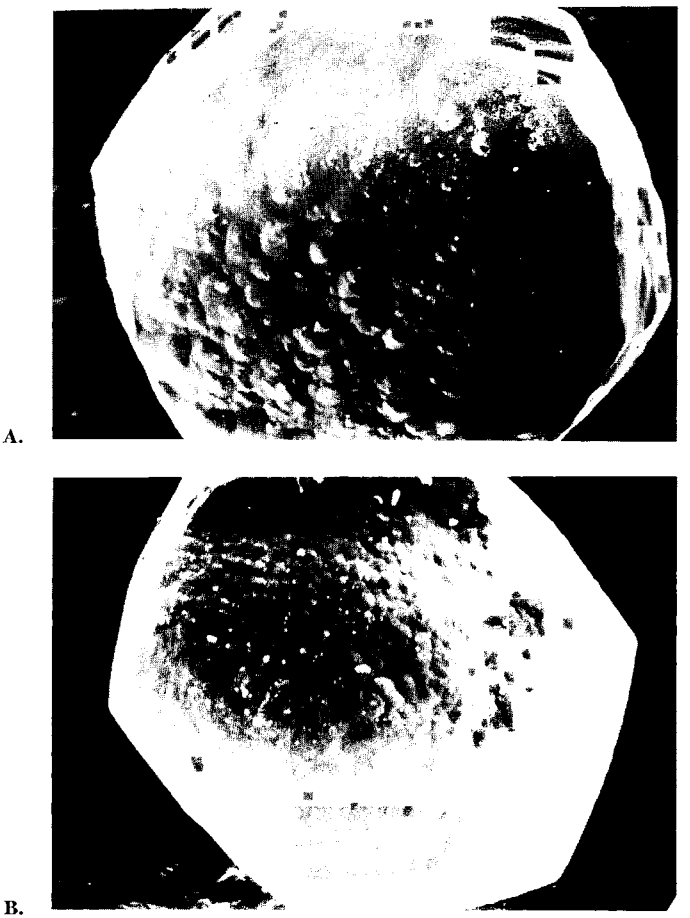

SEM photographs of quartz single crystals. Each crystal has a diameter of approx 1.5mm: (A) unreacted crystal, (B) after dehydration reaction at 700°C and 1 kb for 3 days.

Rate-limiting step.—The mechanism by which the hydration and dehydration reactions take place is a chain mechanism, and the slowest step is therefore rate-limiting. Determination of the rate-limiting step is vital to understanding the factors that control reaction rates in natural systems. There are two possible types of rate-controlling steps: one of the four dissolution or precipitation processes that take place at the mineral-fluid interfaces, or transport of one of the dissolved species through the fluid phase. Reaction at one of the mineral-fluid interfaces may be broken down into a number of component processes (Berner, 1981), but for the purposes of this investigation, it will be dealt with as a single, overall process.

The rate-limiting step of the overall reaction can be investigated using the method of initial rates (Lasaga, 1981a). This technique is based upon the assumption that for an initial period the reaction does not proceed to such an extent that the important variables (surface areas of the solid phases) are significantly changed during the early stages of reaction. If the reaction rate is controlled by a dissolution or precipitation reaction at a particular fluid-solid interface, the rate should be a function of the surface area of that phase. Using the method of initial rates, variation of the surface areas of the individual solid phases in the experiments should reveal such a rate dependence.

The surface areas of the minerals were varied individually by doubling the weight of that mineral in the capsule. Because material of the same grain size as in the previous experiments was used, the surface areas were doubled. Because the weight proportions of minerals in the mix were varied, the spatial configuration of the starting mixture was also altered. Sets of experiments with doubled surface areas of muscovite, sanidine, and andalusite were conducted on both sides of the equilibrium boundary. Experiments in which the surface area of quartz was doubled were conducted on the hydration side of the equilibrium boundary. Because quartz spheres of varying sizes were used in the investigation of the dehydration reaction rates, it was possible to check for a correlation between the amount of reaction and the surface areas of quartz spheres among the three capsules used in each experiment. The surface areas of the quartz spheres, calculated assuming smooth, spherical crystals, varied by as much as a factor of two within the same hydrothermal run. However, no correlation was found between the surface areas of the quartz spheres and measured reaction rates.

During the course of the doubled surface area experiments, some inconsistencies within the data were noted. Repetition of the experiments at 400° and 450°C, 2 kb using equal weights of all starting materials produced different rates than earlier experiments. The discrepancy appeared to affect only the hydration reaction experiments. The experiments with doubled surface areas of andalusite at these two sets of P-T conditions were carried out before the rate change took place. All other experiments, including those with equal weights of the starting materials at other temperatures and pressures, were carried out after the observed change in the reaction rate took place. The precise cause of this rate change is unknown. It is suspected that the composition of the acid solution used to etch the starting materials was inadvertently changed. It was noted in a previous section that the effects of pre-treatment of the starting materials were much greater for the hydration reaction than for dehydration. This would explain why there was no change in the rate of the dehydration reaction, even though the starting mixes were prepared from the same materials. Both sets of data for the equal weights experiments at 400° and 450°C at 2 kb are listed in table 3. For purposes of comparison, the experiments with doubled surface area of andalusite at 400° and 450°C correspond to the equal weights data marked "A" in table 3. All other doubled surface area rates correspond to the data labeled "B." The ratios

TABLE 4
Reaction rates of mixtures with doubled (2x) surface areas of solid phases, divided by rates obtained with equal weights mixtures. Numbers in parentheses are one standard deviation

P (kb)	T°C	2x andalusite	2x sanidine	2x muscovite	2x quartz
2	400	1.672(0.151)	1.215(0.111)	1.037(0.129)	1.135(0.148)
2	450	1.388(0.097)	0.792(0.102)	1.156(0.141)	0.807(0.192)
3	500	1.568(0.147)	1.091(0.119)	1.007(0.080)	1.196(0.126)
1	650	1.874(0.076)	1.284(0.073)	1.658(0.076)	—
2	675	2.651(0.170)	1.003(0.091)	1.049(0.091)	—
1	700	1.592(0.085)	1.138(0.059)	0.916(0.059)	—
average		1.791(0.309)	1.087(0.232)	1.137(0.246)	1.046(0.273)

obtained by dividing the rates of the doubled weight of andalusite experiments by the rates of the equal weights experiments were the same for the 500°C, 3 kb data as for the experiments at 400° and 450°C, 2 kb.

Reaction rates obtained from experiments using doubled weights of the various solids are listed in table 3. The ratios of the rates obtained using doubled weights of the various solid phases and the rates obtained using equal weights of the starting materials appear in table 4. The rates are probably accurate to only ± 25 percent, which is the standard deviation of the averages of the ratios for each solid phase. There appears to be no significant variation in the ratios on either side of the equilibrium boundary or with temperature or pressure. Based on these results, it appears that the hydration and dehydration reaction rates are controlled by the surface area of andalusite, because increasing the surface area of andalusite increased the rate of reaction. Thus, the rate of the net reactions probably was controlled by reaction at the andalusite-fluid interface. However, the rate of mass transfer in the fluid may also be related to the surface area of a solid phase. Variation in the weight proportions of the starting mix altered the spatial configuration of the mix; if transport is the rate-controlling mechanism, such a change in the configuration of the mixture could bring about a change in the reaction rate. The interpretation of rate data obtained in this study therefore required an examination of the physical configuration of the experimental system.

Mixtures used in the hydration experiments were packed into capsules, impregnated with epoxy, and thin-sectioned for examination. In both the equal weights and doubled weights of andalusite mixes, andalusite, K-feldspar, and quartz were completely surrounded by flakes of muscovite. From these thin sections, the configuration of the grains can be modelled as individual blocks of andalusite, K-feldspar, and quartz surrounded by a matrix of muscovite plus fluid.

Because the surface areas of K-feldspar and quartz did not affect the reaction rates, the possibility of rate control by transport of potassium or silica through the fluid phase can be ruled out. Transport of aluminum through the fluid phase or reaction at the andalusite-fluid interface are the

remaining possibilities for the rate-controlling step of reaction (1). The observed configuration of the starting materials indicates that increasing the proportion of muscovite in the mixture only increased the thickness of the muscovite layers around the other components of the mix. This change would not affect the transport of aluminum between muscovite and K-feldspar and between muscovite and andalusite during reaction. Also, if aluminum transport is rate limiting, the surface area of K-feldspar should affect the reaction rate. The lack of dependence of the reaction rate on the feldspar surface area supports rate control by reaction at the andalusite-fluid interface.

Calculated concentration gradients of aqueous species in the fluid may provide additional evidence concerning the identity of the rate-controlling step. If the rate of transport of a dissolved species through the fluid phase is rapid relative to the rate of attachment or detachment of ions at one of the fluid-solid interfaces, the concentration gradients of dissolved species will be very small. The concentrations of aqueous species will therefore be close to equilibrium with the minerals that have fast interface reaction rates (fig. 7A). If the rate of transport of a particular dissolved species through the fluid phase is slower than the reaction rates at the mineral-fluid interfaces, then the concentrations of that dissolved species will build up to nearly saturation levels at the dissolving mineral interfaces, while the concentrations will drop to values near equilibrium at the surfaces of the precipitating phases (fig. 7B). This is the "local equilibrium" condition. A concentration gradient will therefore form between the dissolving and precipitating phases. The possibility also exists of an intermediate situation, where transport of one of the dissolved species takes place at nearly the same rate as one of the interface reactions (fig. 7C). In such a situation, the concentration gradient will be intermediate between the cases of interface-reaction and transport rate control.

If transport of aluminum between muscovite and andalusite is indeed the rate-controlling step of reaction (1), the concentration gradient may be estimated by calculating the difference between the concentrations of aluminum in equilibrium with andalusite and muscovite and dividing by

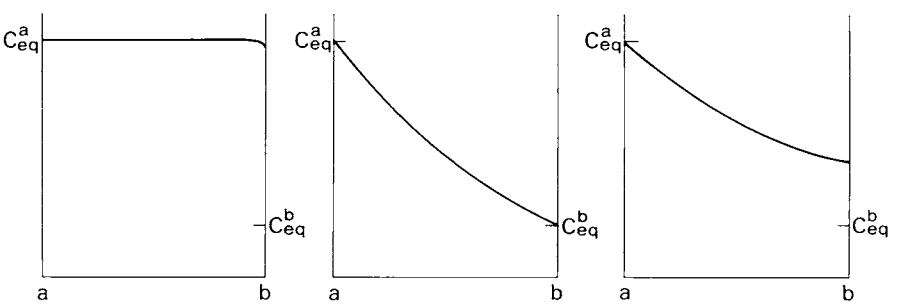

Fig. 7. Schematic concentration gradients for reactions with different rate-controlling steps (after Berner, 1980).

the distance over which transport of aluminum takes place. This assumes a linear concentration gradient.

The dissolution reactions for andalusite and muscovite may be written as:

$$Al_2SiO_{5(s)} + 3H_2O \rightleftarrows 2Al(OH)_{3(aq)} + 3SiO_{2(aq)} \quad (7)$$

$$KAl_3Si_3O_{10}(OH)_{2(s)} + H^+_{(aq)} + 3H_2O \rightleftarrows K^+_{(aq)} + 3Al(OH)_{3(aq)} + 3SiO_{2(aq)} \quad (8)$$

The ΔG_f° of minerals and aqueous species were calculated with the data of Helgeson and others (1978), Helgeson, Kirkham, and Flowers (1981), and Helgeson and Kirkham (1974), with the exception of ΔG_f° for $Al(OH)_{3(aq)}$, which was obtained from Ragnarsdottir and Walther (1985). Because pure H_2O was the initial fluid, and reaction (1) does not produce or consume $H^+_{(aq)}$, the pH used in the calculation was neutral, adjusted for pressure and temperature. The concentration of silica in solution was set equal to the solubility of quartz (Fournier and Potter, 1982), and the calculations were carried out for congruent dissolution. At 450°C and 2 kb, $C^{eq}_{Al(OH)^\circ_3,\,musc} = 1.9 \times 10^{-5}$ molal and $C^{eq}_{Al(OH)^\circ_3,\,and} = 8.1 \times 10^{-5}$ molal, which means that the difference in concentration of the solutions in equilibrium with the two minerals is 6.2×10^{-5} molal. If, as may be estimated from the thin section of the starting materials, the maximum distance over which aluminum must be transported between the muscovite and andalusite is 1×10^{-4} cm, the gradient calculated between the two minerals for the case of rate control by aluminum diffusion is 0.62 molal/cm.

The actual concentration gradients present during the experiments may be estimated in the following manner. It is known that:

$$\frac{dn_i}{dt} = J_j A_i \nu_{ij} \quad (9)$$

and, from Fick's first law,

$$J_j = -D_j \left.\frac{dC_j}{dx}\right|_{x=0} \quad (10)$$

assuming one-dimensional diffusion perpendicular to the mineral surfaces. J_j is the flux of species j, ν_{ij} is the moles of i per mole of j, D_j is the diffusion coefficient of j, n_i is moles of phase i, A_i is the surface area of phase i, and C_j is the concentration of species j in the fluid. The rates (dn_i/dt) were measured in the rate experiments. The surface areas of the solids in the starting mixtures were determined from gas adsorption isotherm measurements (table 5). The surface areas of the spherical quartz single crystals were estimated from a measured diameter of 0.2 cm and assuming a perfect spherical shape. The fluxes of the various components at the surface of each mineral were thus calculated as follows. The diffusion coefficient for $Al(OH)_{3(aq)}$ at 450°C, 2 kb was estimated from the diffusion coefficient for $SiO_{2(aq)}$ measured at 550°C, 1 kb (Ildefonse and Gabis, 1976) using the Nernst-Einstein equation (Nigrini, 1970):

$$\left(\frac{D_j^\circ \eta_{H_2O}^\circ}{T_1}\right)_{P_1} = \left(\frac{D_j^\circ \eta_{H_2O}^\circ}{T_2}\right)_{P_2}, \qquad (11)$$

where D_j° is the tracer diffusion coefficient of j, and $\eta_{H_2O}^\circ$ is the viscosity of pure water. The viscosity of water at 450°C and 2 kb was obtained from Todheide (1972). At these conditions, the calculated diffusion coefficient for $SiO_{(aq)}$, and hence, $Al(OH)_{3(aq)}$ was 1.3 x 10^{-4} cm²/sec, the calculated flux for $Al(OH)_{3(aq)}$ at the andalusite surface was -1.6 x 10^{-11} moles/cm² sec, and the resultant concentration gradient was 1.7 x 10^{-4} molal/cm.

The aluminum gradient calculated for the case of rate control by aluminum transport between andalusite and muscovite was 0.62 molal/cm at 450°C and 2 kb, which is much greater than the value calculated from the flux at the andalusite surface. The calculated aluminum gradient that apparently existed in the fluid during reaction was, therefore, significantly smaller than the gradient expected for rate control by transport through the fluid phase. Thus, aluminum transport was not the rate-controlling step of reaction (1).

Another potential means of distinguishing between two rate-controlling mechanisms is by modelling the amount of reaction as a function of time and examining the agreement of the observed data with the different models. However, because both potential rate-controlling steps in this reaction, aluminum transport and reaction at the andalusite surface, are dependent on the surface area of andalusite, the two cannot be distinguished by this means.

Further indication of the rate-controlling step for the hydration and dehydration reactions may be obtained from textural features of the run products. Berner (1978) observed that when the rate of a dissolution process is controlled by transport through the fluid phase, the surface of the dissolving mineral is typically smooth, with no evidence of crystallographic control of the surface morphology. The smooth texture is caused by the rapid rate of detachment of surface material, which makes preferential dissolution of high-energy sites unlikely. If, on the other hand, the rate is controlled by reaction at the mineral-fluid interface, the surface of the dissolving mineral will exhibit crystallographically controlled features (for example, etch pits). This surface texture is the result of the relative difficulty of removal of ions from the mineral surface; the high-energy sites are therefore preferentially removed (Lasaga and Blum, 1986). SEM examination of andalusite grains from hydration

TABLE 5

Specific surface areas of solid starting materials. Minerals sieved to between 325 and 400 mesh. Muscovite ultrasonically washed only; all other solid starting materials etched in acid solution and washed ultrasonically

Muscovite	10447 ± 365 cm²/g
Quartz	846 ± 46
Andalusite	836 ± 45
Sanidine	891 ± 105

TABLE 6
Equilibrium brackets used for ΔG_R calculations

Author	T_{eq} (P = 2 kb)
Evans (1965)	600 ± 10°C
Althaus and others (1970)	622 ± 10
Kerrick (1972)	605 ± 10
Day (1973)	640 ± 10
Chatterjee and Johannes (1974)	597.5 ± 7.5
This study	601 ± 45

experiments in which andalusite dissolved reveal surface morphologies that are angular and that appear to have some measure of crystallographic control (pl. 3-B), that is, rows of angular protrusions, sharp corners, and occasional pitting of the surface were common. The textural evidence is therefore consistent with control of the rate of hydration by reaction at the andalusite-fluid interface.

Andalusite grains observed in the run products of the dehydration reaction (pl. 3-C) typically have extremely jagged, irregular surfaces. These textures indicate rate control by the precipitation process at the andalusite-fluid interface, because if transport is the rate-controlling step, the andalusite grains should be smooth and rounded.

Dependence of reaction rate on free energy of reaction.—The net reaction rate (R_{net}) of reaction (1), as written, is the dehydration rate minus the rate of the hydration reaction:

$$R_{net} = R_D - R_H, \tag{12}$$

where R_D and R_H are the rates of dehydration and hydration, respectively. Because of the dependence of the rates on the andalusite surface area, the reaction rates were normalized by dividing by the surface area of andalusite. From transition state theory (Lasaga, 1981b):

$$\frac{R_D}{R_H} = e^{-n\Delta G_R/RT}, \tag{13}$$

which, when substituted into eq (13) yields:

$$R_{net} = R_D (1 - e^{n\Delta G_R/RT}). \tag{14}$$

Therefore, if a value for n is assumed, the rate of the dehydration reaction may be calculated from the measured values of R_{net} and calculated values of ΔG_R at various sets of P-T conditions.

If an Arrhenius dependence of the dehydration rate on temperature is assumed, then:

$$R_D = B_o e^{-E_D/RT}. \tag{15}$$

Taking the logarithm of both sides of eq (15):

$$ln\ R_D = ln\ B_o - \frac{E_D}{RT} \tag{16}$$

If B_o and E_D are not functions of temperature, then $ln\ R_D$ is a linear function of inverse temperature. The slope of this line is the apparent

activation energy of the dehydration reaction divided by the gas constant, and the intercept is the natural logarithm of the "pre-exponential factor," B_o.

To determine the free energy of reaction (ΔG_R), an equilibrium temperature was obtained from a linear least-squares fit of the reaction rates at 500°, 600°, and 650°C, 2 kb versus temperature. The equilibrium temperature obtained in this manner is 601°C. A standard deviation about this equilibrium temperature of ± 22°C was obtained graphically from a plot of the standard deviation about the line. In spite of this relatively large error, the equilibrium brackets obtained by Evans (1965), Kerrick (1972), and Chatterjee and Johannes (1974) (table 6) are in agreement with the equilibrium temperature calculated from the 2 kb rate data. The results of Althaus and others (1970) and Day (1973) are at much higher temperatures than the equilibrium temperature indicated by the rate data. The mean of the stated uncertainties from Evans (1965), Kerrick (1972), and Chatterjee and Johannes (1974) was therefore used to estimate the uncertainty of the equilibrium temperature obtained in this study. The equilibrium temperature of 601°C was used with the heat capacity equations of the phases from Robie, Hemingway, and Fisher (1978) to calculate ΔG_R. The uncertainty of the calculated ΔG_R was obtained from the equation (Anderson, 1977):

$$\sigma_{\Delta G_R} = \Delta T \Delta S_R, \tag{17}$$

where ΔT is the width of the equilibrium bracket. The calculated values of ΔG_R, $\sigma_{\Delta G_R}$, and the values of R_{net} in moles/cm² sec are listed in table 7. Use of the 500°, 600°, and 650°C data at 2 kb to calculate the equilibrium temperature, assuming a linear dependence of the reaction rate on temperature, was corroborated by the calculated ΔG_R values obtained at these experimental conditions: the absolute value of ΔG_R is less than the quantity RT, which is necessary for the nearly linear relationship of reaction rate to temperature, as required by eq (14).

Natural logarithms of the rates of the dehydration reaction (R_D) were calculated from the data listed in table 7, assuming a value of n = 1 as a first approximation (Fisher and Lasaga, 1981). The fit to these data was obtained with a weighted least-squares linear regression as a function of inverse temperature. The data and best-fit line are illustrated in figure 8. The activation energy obtained was 51.4 ± 12.2 KJ/mol. The linear correlation coefficient obtained was r = 0.84, but the best-fit line does not describe adequately the low temperature behavior of the reaction rate. At 350°C and 2 kb, the reaction rate predicted by the best-fit line is over four times the experimentally observed reaction rate. If the net rate at 150°C and 2 kb is calculated, it equals -4.7×10^{-12} moles/cm² sec, which is much higher than would be expected at such a low temperature. Values of n from 0.1 to 10 did not improve the fit to the data. A possible explanation for the poor fit to the data at low temperatures is the assumption that the activation energy is independent of temperature over the range studied. Over relatively large temperature ranges, the activation energy may be a function of temperature. Substitution of various polynomial functions of

TABLE 7

Calculated ΔG_R, $\sigma_{\Delta G_R}$, and measured net reaction rates normalized to the andalusite surface area

P (kb)	T(°C)	R_{net} (moles H_2O/cm² sec)	σ_{Rnet}	ΔG_R(Joules/mole)	$\sigma_{\Delta G_R}$
2	350	-9.3035×10^{-13}	6.3131×10^{-13}	15253.0	4586.8
2	400	-6.5072×10^{-12}	4.9397×10^{-13}	12240.0	4512.3
2	400	-3.6239×10^{-12}	2.5595×10^{-13}	12240.0	4512.3
2	450	-7.9860×10^{-12}	7.0220×10^{-13}	9210.6	4437.3
2	450	-4.7107×10^{-12}	1.9753×10^{-13}	9210.6	4437.3
2	500	-1.6121×10^{-12}	1.3936×10^{-13}	6176.7	4362.1
3	500	-2.2994×10^{-11}	1.0814×10^{-12}	8049.1	4362.1
1	600	5.5378×10^{-13}	3.5442×10^{-14}	-3023.0	4198.1
2	600	-2.3037×10^{-14}	4.9614×10^{-14}	59.5	4198.1
1	650	1.3455×10^{-12}	3.7722×10^{-14}	-6497.4	4140.7
2	650	8.9287×10^{-13}	7.2962×10^{-14}	-2971.3	4140.7
2	675	2.6630×10^{-12}	1.6126×10^{-13}	-4494.9	4113.1
1	700	7.6785×10^{-12}	3.7435×10^{-13}	-10010.0	4086.3

temperature for the activation energy in eq (16) did not significantly improve the fit to the data, probably because of the relatively large amount of scatter in the data. Another possible reason for the poor fit to the data is a change in the reaction mechanism.

It is expected that the characteristics of the solid phases (for example, composition, stacking order, Al/Si order-disorder) would affect the

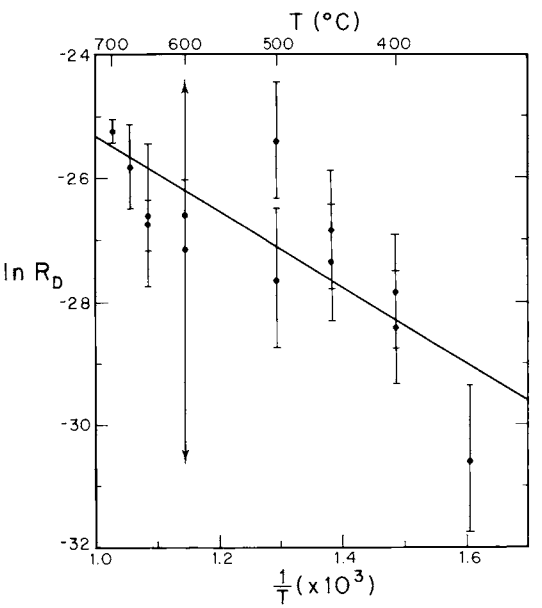

Fig. 8. Plot of the logarithm of the dehydration rate versus 1/T. R_D is in units of (moles/cm² andalusite/sec).

reaction rate because of the corresponding change in the free energy of reaction. To examine the effect of ΔG_R on the reaction rate, a series of experiments were conducted at 450°C and 2 kb that were identical to the earlier rate experiments, except that sanidine was replaced by adularia (see section on starting materials). Although the adularia was not completely ordered, the difference in Al/Si disorder between the two feldspars was substantial. The results of experiments using the relatively ordered and disordered forms of the feldspar are compared in figure 9 and listed in table 3. The reaction rate was significantly reduced when adularia was substituted for sanidine in the starting mixture. The net reaction rate measured in the experiments on the adularia-bearing mixture was used to calculate the free energy of reaction, using eq (2) and the best-fit values for the pre-exponential factor and activation energy as discussed above. The difference in the free energy of reaction when adularia is substituted for sanidine was calculated to be approx 1 KJ/mol. If the adularia was completely ordered, a difference of approx 5 KJ/mol would be expected in ΔG_R, as calculated from the thermodynamic data of Robie, Hemingway, and Fisher (1978). The magnitude and direction of the rate change is therefore reasonably consistent with the intermediate state of the Al/Si ordering of the adularia.

The change in reaction rate encountered with the variation in the Al/Si order-disorder of the feldspar demonstrates that the nature of the phases involved in the reaction can significantly affect reaction rates. The

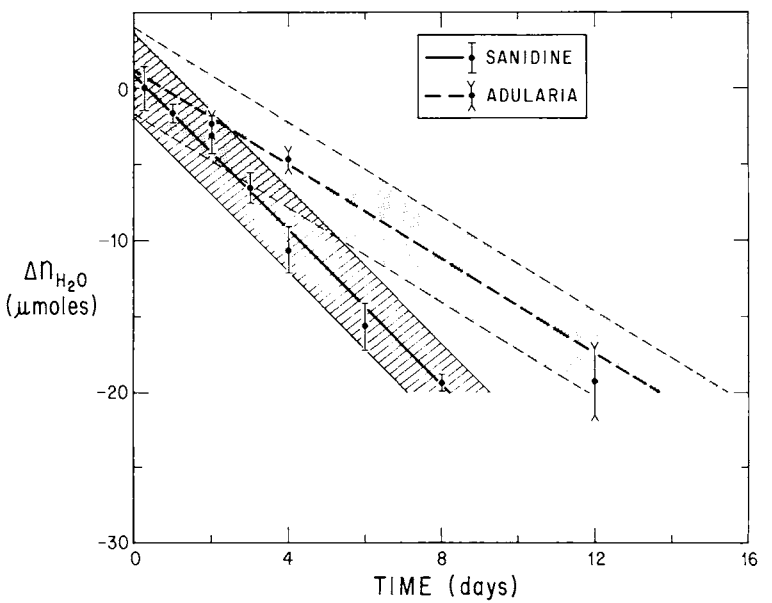

Fig. 9. Comparison of the results of experiments conducted with starting mixtures that contained either adularia or sanidine at 450°C and 2 kb.

TABLE 8

Values of ΔG_R calculated at P-T conditions of hydration experiments. One set of values was calculated using thermodynamic data ($2M_1$ muscovite). The other set of values was calculated from the net reaction rates, with the activation energy and pre-exponential factor from the net dehydration data. The second set of ΔG_R values presumably includes the effects of the 1M muscovite

E_D = 189(± 53) KJoule /mol
B_o = 0.150(± 0.9898) moles/cm² sec

P(kb)	T(°C)	ΔG_R($2M_1$ muscovite) (KJoule/mol)	ΔG_R(1M and $2M_1$ muscovite) (KJoule/mol)
2	350	15.3	55.5
2	400	12.2	55.6
2	400	12.2	52.4
2	450	9.2	46.9
2	450	9.2	43.8
2	500	6.2	26.9
3	500	8.0	43.9
2	600	0.1	0.2

muscovite produced by the hydration reaction may have been a mixture of $2M_1$ and 1M muscovite, which is not the same as the pure $2M_1$ muscovite in the starting materials. The hydration reaction that involved the disordered muscovite should have a smaller ΔG_R, when written as a dehydration reaction, than the same reaction with pure $2M_1$ muscovite as a product phase. The change in ΔG_R could account for the poor fit of eq (16) to the low-temperature data.

Eq (16) was fit to the dehydration rates calculated from the net dehydration data. This rate data should correspond to reaction (1) with $2M_1$ muscovite only, because no 1M muscovite was detected in the run products of the dehydration experiments. The values of the activation energy and pre-exponential factor obtained for the dehydration reaction, $E_D = 189 \pm 53$ KJ/mol and $B_o = 0.150 \pm 0.990$ moles cm² sec, and the rates measured in the experiments were used in eq (3) to calculate ΔG_R values at the P-T conditions of the net hydration experiments. The values of ΔG_R calculated in this manner are listed in table 8 with values of ΔG_R calculated from the thermodynamic data for reaction (1) with $2M_1$ muscovite. The standard deviations of the values of ΔG_R calculated from the net hydration rate data are about as large as the ΔG_R values. The direction of the change in ΔG_R, however, should be accurate. The shift in ΔG_R is in the wrong direction to be caused by the involvement of 1M muscovite in the reaction. The poor fit of eq (16) to the low-temperature data is therefore probably due to the dependence of the activation energy on temperature.

The activation energy expected if the reaction rate is controlled by transport through the fluid phase is approx 20-25 KJ/mol (Lasaga, 1981a). The activation energy obtained, 51.4 ± 12.2 KJ/mol using all of the rate data, or 189 ± 53 KJ/mol using only the net dehydration data, is outside this range. Other studies have established that the rates of most silicate

dissolution reactions are controlled by processes at the mineral-fluid interface (Berner, 1978; Lasaga, 1981a). The activation energies obtained for these silicate dissolution processes are in the range of 30 to 150 KJ/mol (Lasaga, 1981a). The activation energy values obtained in this study are comparable to these values and are therefore consistent with the identification of the rate-limiting step of reaction (1) as the dissolution and precipitation processes at the andalusite-fluid interface.

The rate law.—From the values of the reaction rates as functions of the surface areas of the starting materials (table 4), there is little indication of a change in the rate-controlling mechanism as a function of temperature and pressure. Reaction rates at a given pressure and temperature appear to be principally controlled by the surface area of andalusite. With few exceptions, the rates of reaction in the experiments with doubled surface areas of muscovite, sanidine, and quartz are within $\pm 2\sigma$ of the rates obtained in the experiments with equal weights of all starting materials.

An empirical form for the rate law for a reaction (Lasaga, 1981a, 1984) is:

$$\frac{1}{\nu}\frac{dC_A}{dt} = k\, C_A^{n_a}\, C_B^{n_b} \ldots, \tag{18}$$

where the variable C_j represents some units of concentration, the variables n_i are any real numbers, and ν is a stoichiometric coefficient. For heterogeneous reactions, the concentration units may be replaced by surface areas of the solid phase or phases involved. The stoichiometric coefficients for reaction (1) are equal to 1, and in the experiments of this study only the surface area of andalusite affected the reaction rate. Therefore, the rate equations for the hydration and dehydration reactions may be written:

$$R_H = k_H\, A_{and}^{n''}, \tag{19}$$

and

$$R_D = k_D\, A_{and}^{n'} \tag{20}$$

where R_D and R_H are in units of moles/cm^2 sec. The values of n' and n'' for the hydration and dehydration reactions may be calculated from the rates in experiments conducted with equal weights of all starting materials and from those in which the weight of andalusite was doubled (table 3). The values of n' and n'' so obtained are listed in table 9. The mean value of n'' for the hydration experiments is 0.62, with a standard deviation of 0.22. The mean value of n' for the dehydration reaction is 1.00, with a standard deviation of 0.14. The value of n' obtained from the dehydration experiments is probably more accurate, because of the greater precision of the Δn_{qtz} measurements. From the data in table 4, there is no indication of a difference in the dependence of reaction rate on the surface area of andalusite between the hydration and dehydration reactions. Therefore, the best value of the exponent is probably equal to 1 for both the hydration and dehydration reactions. In the presence of a pure aqueous phase, the rate law for the dehydration reaction can therefore be written:

$$R_D = k_D A_{and} \quad , \tag{21}$$

and for the dehydration reaction, it is:

$$R_H = k_H A_{and} \quad . \tag{22}$$

Reaction in mixed volatiles.—The rates of the hydration and dehydration reactions are expected to be functions of the fugacity of H_2O because of the effect of fugacity on ΔG_R at constant P and T. Based only on the change in ΔG_R as a function of f_{H_2O}, it was expected that the rate of the dehydration reaction would be increased by a decrease in f_{H_2O}. The reaction rate observed in the mixed H_2O-CO_2 experiments was less than the rate observed at the same pressure and temperature conditions in pure H_2O (fig 6 and table 3).

X-ray diffraction and SEM observation of run products from the mixed-volatile experiments revealed that the aluminum-silicate produced by the reaction was a fibrous aluminum-silicate, either sillimanite or mullite, rather than the andalusite polymorph produced by the reaction in pure water. It is extremely difficult to differentiate between these two phases on the basis of powder diffraction data, particularly within a mixture of other phases. Using the criteria of Carr and Fyfe (1960), however, the aluminum-silicate was tentatively identified as mullite. The aluminum-silicate appeared to nucleate and grow primarily on the surfaces of the andalusite grains present in the starting mixtures (pl 6). Nucleation and growth of the aluminum-silicate were observed in the run products of one experiment in pure H_2O at 700°C and 1 kb. This instance of the growth of the aluminum-silicate in pure H_2O may indicate that only a small amount of CO_2 would be necessary to promote the growth of mullite over andalusite.

Because a new phase was produced by the dehydration reaction in an H_2O-CO_2 fluid, it is impossible to compare rigorously the data obtained in pure water versus mixed volatiles. Qualitatively, however, it is evident that the change in fluid composition decreased the dehydration reaction rate. The overall reaction mechanism appears unchanged, with product phases precipitating on the preexisting product grains.

TABLE 9
n′ and n″ values calculated from hydration and dehydration data

HYDRATION		
P (kb)	T (°C)	n″
2	400	0.74(0.13)
2	450	0.47(0.10)
3	500	0.65(0.14)
DEHYDRATION		
P (kb)	T (°C)	n′
1	650	0.91(0.06)
2	675	1.41(0.10)
1	700	0.67(0.08)

PLATE 6

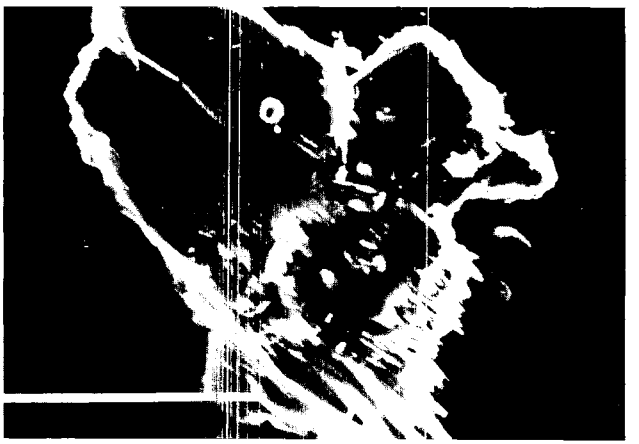

SEM photograph of an andalusite grain with fibrous aluminum-silicate overgrowths after dehydration reaction at 700°C and 1 kb with X_{CO_2}=0.48, for 3 days.

Applications to natural systems.—Wood and Walther (1983) examined the rates of some metamorphic reactions, as determined from equilibrium studies carried out using single-crystal techniques. They reasoned that in single crystal experiments, the reaction rate should be controlled by the rate of the dissolution or precipitation process at the interface of the single crystal. This assumption was based on the small surface area of the crystal relative to the surface areas of the powdered starting materials. However, in the dehydration experiments of this study, the reaction rate was independent of the surface areas of the quartz single crystals. The reaction rate was instead solely dependent on the surface area of andalusite. Wood and Walther's assumption should be valid only if the specific rates of reaction at the various mineral-fluid interfaces are of the same order of magnitude. Based on the results of the present study, the specific rate of the andalusite interface reaction is much less than the specific rate of reaction at the quartz interface.

If k_D (units of g atom oxygen/cm^2 sec), the rate constant for the dehydration reaction, is obtained from the net rate divided by the surface area of the quartz, the data in this study for the dehydration reaction rate are in good agreement with the equation determined by Wood and Walther (1983) (fig. 10). If, as justified by the results of this study, the rate constant k_D is calculated assuming rate control by reaction at the andalusite-fluid interface, the results illustrated as circles in figure 10 are obtained. Although these data roughly parallel the line determined in the Wood and Walther (1983) study, they do not agree with their predictions. The probable reason for the similarity in slopes is that the calculation outlined by Wood and Walther (1983) is very similar to the calculation of activation

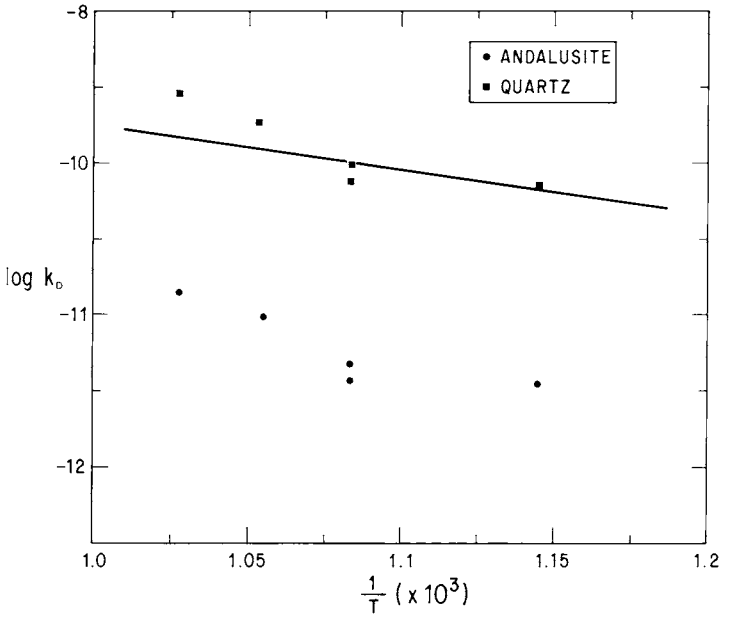

Fig. 10. Logarithms of k_D (oxygen g atom/cm^2 sec) versus 1/T, calculated assuming reaction at quartz single crystal-fluid interface is rate-controlling (squares) and assuming reaction at andalusite-fluid interface is rate-controlling (circles). The line in this diagram is the best-fit line obtained by Wood and Walther (1983).

energies discussed in the previous sections. The rate-controlling mechanism of most metamorphic reactions involving silicate minerals in experimental systems is probably dissolution or precipitation process at a mineral-fluid interface. The apparent activation energies of silicate metamorphic reactions in the presence of excess fluid should therefore lie within a narrow range (Lasaga, 1984). Wood and Walther (1983) further stated that "fluid composition does not appear to be an important factor in the high temperature region." The results of the mixed-volatile experiments in this study indicate that fluid composition may affect reaction rates.

Considerable care must be exercised in applying the results of this study to the rates of reactions in natural processes. The experiments in this study were carried out on ground, fine-grained mixtures of reactants and products in the presence of a relatively pure aqueous fluid, a situation unlikely to occur in nature. However, in this study the reaction rates were normalized to the surface area of andalusite. Thus, unless the grain boundary region is quite small and the amount of fluid is also small, so that the reaction rate is controlled by the rate of diffusion, the results of this study should be applicable to reactions in the presence of an aqueous phase. The presence of reactants and products in the starting mixture eliminated the effects of nucleation of product phases and may have

profoundly influenced reaction rates. For example, if the nucleation of a product phase is sluggish, the rate of the overall reaction would be reduced. However, nucleation experiments in this system (Schramke, Kerrick and Lasaga, in preparation) indicated that nucleation occurs readily.

If, in a natural system, product phases nucleate on the surface of a reactant phase and form a coherent boundary layer, the reaction rate will undoubtedly be controlled by the rate of diffusion through this product layer. The results of this study would not apply to such a situation. If "armoring" does not occur, however, reaction in the presence of a fluid probably proceeds by dissolution of reactant phases, transport of dissolved material through the fluid phase, and precipitation onto product grains.

This study indicates that in the presence of excess fluid the rate-limiting step of such a reaction will be reaction at the interface of one of the minerals with the fluid. The control of reaction rates by the reaction at a mineral-fluid interface is even more probable in nature, because during metamorphism devolatilization reactions commonly occur, thereby promoting the flow of fluids through the rock unit. The result would be an increase in the rate of transport of dissolved material, making rate control by reaction at a mineral-fluid interface more likely. Furthermore, Berner (1978) pointed out that in natural systems, the fluid phase typically contains dissolved material that may adsorb onto the active sites on mineral surfaces, making reaction at the mineral-fluid interface slower, and thereby increasing the likelihood of rate control by reaction at the mineral-fluid interface.

If, in nature, the hydration and dehydration reactions take place via the dissolution-transport-precipitation mechanism described in this study, the experimentally measured rates for reaction (1) may be applied to the same reaction in natural systems. For example, the andalusite was assumed to be present initially as rectangular blocks of height and width equal to w_o and length equal to $2w_o$. For the hydration reaction (andalusite dissolution), the length l (cm), and width w (cm) of an andalusite grain are:

$$w = w_o - 2kt \tag{23}$$

$$l = 2w_o - 2kt, \tag{24}$$

if isotropic dissolution is assumed, and if dissolution is proportional to time. The rate constant is k (cm/sec). The factor of two appears in eq (23) and (24) because the grains dissolve on two sides. From (23) and (24):

$$\frac{dw}{dt} = \frac{dl}{dt} = -2k \quad . \tag{25}$$

From the equation for the volume of the andalusite grain:

$$\frac{dV_{and}}{dt} = 2lw\frac{dw}{dt} + w^2\frac{dl}{dt} \quad . \tag{26}$$

Substituting (23)-(25) into (26):

$$\frac{dV_{and}}{dt} = -10\,k w_o^2 + 32\,k^2 w_o t - 24\,k^3 t^2 \quad , \tag{27}$$

Integrating from V_o, the volume at time = 0, to V, the volume at time t:

$$\Delta V = -10\,k w_o^2 t + 16\,k^2 w_o t^2 - 8\,k^3 t^3 \quad , \tag{28}$$

where ΔV is the change in volume, $V\text{-}V_o$. Similarly, for the dehydration reaction:

$$\Delta V = 10\,k w_o^2 t + 16\,k^2 w_o t^2 + 8\,k^3 t^3 \quad . \tag{29}$$

Reaction (1) should take place during contact metamorphism if the pressure is less than about 2 kb (Turner, 1981). Using eq (29), the time necessary for the hydration reaction (1) to consume andalusite crystals of various initial dimensions was calculated. The value of k was obtained using eq (2) with the activation energy and pre-exponential factor previously obtained by fitting eq (16) to all the rate data. Table 10 lists the amount of time necessary for the complete consumption of the different size crystals at various temperature intervals below the 2 kb equilibrium boundary. At a temperature 26°C below the equilibrium boundary, even a relatively large (2 cm^3) crystal of andalusite should be consumed by the hydration reaction (1) in 950 yrs. At conditions very close to the equilibrium boundary, 600°C and 2 kb, the reaction times are increased but still relatively short on a geologic scale. It is therefore likely that, unless water is removed from the system, the hydration reaction (1) should completely consume the high-temperature assemblage during the cooling stages of contact metamorphism.

Judging from Jaeger's (1957, 1959) calculated thermal profiles about an intrusion and assuming $P_{H_2O} = P_{total}$, dehydration reaction (1) in contact aureoles should take place only if the temperature of the intruding magma is high or if the initial temperature of the country rock is elevated. The dehydration reaction should also be generally restricted to an area near the intrusive contact, because of the relatively high temperatures required: greater than 600°C at 2 kb. If such temperatures are attained, however, reaction should quickly proceed to completion. Dehydration reaction (1) should be more common in contact aureoles if $P_{H_2O} < P_{total}$. Although $P_{H_2O} < P_{total}$ appears to reduce the reaction rate (fig. 6), the measured rate was still relatively rapid.

The amount of time necessary for the dehydration reaction to proceed, starting with muscovite + quartz + andalusite, was calculated in a manner similar to that for the hydration reaction. The calculations were carried out using eq (30), and the values of k were obtained from eq (3) in the manner described for calculations involving the hydration reaction. Various initial grain sizes were assumed for andalusite, and the amount of time necessary to double the volume of andalusite was calculated. The values of the required amount of time are listed in table 10 for temperatures 2° and 24°C above the equilibrium boundary at 2 kb. Even at only 2°C above the equilibrium boundary, it is evident from the calculated amount of time for the size of the andalusite grain to double that the reaction should quickly proceed to completion.

TABLE 10
Time necessary for the volume of an andalusite crystal to vary by a factor of two at various P-T conditions and for different initial sizes of andalusite crystals

			time (years)		
P (kb)	T(°C)	ΔT(°C)*	w_o = 1 cm**	w_o = 0.1 cm	w_o = 0.01 cm
2	500	-100	240	24	2.4
2	575	-26	950	95	9.5
2	600	-1	17,000	1700	170
2	603	+2	1100	110	11
2	625	+24	110	11	1.1
2	650	+49	48	4.8	0.5

*ΔT is the distance of the stated P-T conditions from the equilibrium boundary.
**w_o is the width of andalusite grain.

These calculations assume that the rate-controlling step remains unchanged throughout the reaction progress. As one of the reactants becomes scarce, it is likely that the rate-controlling step will become the dissolution of this relatively scarce phase. Such a change in the rate-controlling step may ultimately slow the disappearance of the unstable mineral assemblage.

CONCLUSIONS

Reaction rates in this study appear to be controlled by reaction at the interface of andalusite with the fluid. Rate control by this step is the result of the observed reaction mechanism, which involves four dissolution-precipitation processes linked by transport through the fluid phase. Control of silicate reaction rates by processes that take place at the mineral-fluid interface is consistent with the rate control of dissolution of silicates by this step in the dissolution mechanism (Berner, 1978). The results of this study indicate that silicate dissolution and precipitation processes are controlled by reaction at the mineral-fluid interface over a wide range in pressure and temperature.

ACKNOWLEDGMENTS

This study represents a portion of the doctoral work of J. A. Schramke and was supported in part by a grant from the Earth Sciences Section of the National Science Foundation (Grant EAR 80-26078), by an Owens-Corning Fiberglas Graduate Fellowship to J. A. Schramke, and by funds provided by Battelle, Pacific Northwest Laboratories. The Harvard Mineralogical Museum (Carl Francis, Curator) provided the muscovite that was used in the experiments. This work was greatly improved by the reviews and comments of H. L. Barnes, R. L. Erikson, F. Helfferich, D. C. Rubie, and J. V. Walther.

REFERENCES

Althaus, E., Karotke, E., Nitsch, K. H., and Winkler, H. G. F., 1970, An experimental re-examination of the upper stability limit of muscovite plus quartz: Neues Jahrb. Mineralogie Monatsh., v. 7, p. 325-336.

Amouric, M., and Baronnet, A., 1983, Effects of early nucleation conditions on synthetic muscovite polytypism as seen by high resolution transmission electron microscopy: Phys. Chem. Minerals, v. 9, p. 146-159.

Anderson, G. M., 1977, Uncertainties in calculations involving thermodynamic data, *in* Greenwood, H. J., ed., Short Course in the Application of Thermodynamics to Petrology and Ore Deposits: Toronto, Mineralog. Assoc. Canada, v. 2, p. 199-215.

Appleman, D. E., and Evans, H. T., 1973, Job 9214: Indexing and least-squares refinement of powder diffraction data: Nat'l. Tech. Inf. Service Doc. PB 216188, Springfield, Va., U.S. Dept. Commerce.

Berner, R. A., 1978, Rate control of mineral dissolution under earth surface conditions: Am. Jour. Sci., v. 278, p. 1235-1252.

———— 1981, Kinetics of weathering and diagenesis, *in* Lasaga, A. C., and Kirkpatrick, R. J., eds., Kinetics of Geochemical Processes, Reviews in Mineralogy, v. 8: Washington D.C., Mineralog. Soc. America, p. 111-134.

Bevington, P. R. 1969, Data Reduction and Error Analysis for the Physical Sciences: New York, McGraw-Hill Book Co., 336 p.

Carr, R. M., and Fyfe, W. S., 1960, Synthesis fields of some aluminum silicates: Geochim. et Cosmochim. Acta, v. 21, p. 99-109.

Chatterjee, N. D., and Johannes, W., 1974, Thermal stability and standard thermodynamic properties of synthetic $2M_1$-muscovite, $KAl_2[AlSi_3O_{10}(OH)_2]$: Contr. Mineralogy Petrology, v. 48, p. 89-114.

Day, H. W., 1973, The high temperature stability of muscovite plus quartz: Am. Mineralogist, v. 58, p. 255-262.

Evans, B. W., 1965, Application of a reaction-rate method to the breakdown equilibria of muscovite and muscovite plus quartz: Am. Jour. Sci., v. 263, p. 647-667.

Fisher, G.W., and Lasaga, A. C., 1981, Irreversible thermodynamics in petrology, *in* Lasaga, A. C., and Kirkpatrick, R. J., Kinetics of Geochemical Processes, Reviews in Mineralogy, v. 8: Washington, D.C., Mineralog. Soc. America, p. 171-185.

Fisher, J. R., and Zen, E-A, 1971, Thermochemical calculations from hydrothermal phase equilibrium data and the free energy of H_2O: Am. Jour. Sci., v. 270, p. 297-314.

Fournier, R. O., and Potter, R. W., 1982, An equation correlating the solubility of quartz in water from 25° to 900° at pressures up to 10,000 bars: Geochim. et Cosmichim. Acta, v. 46, p. 1969-1973.

Fyfe, W. S., Turner, F. J., and Verhoogen, J., 1958, Metamorphic reactions and metamorphic facies: Geol. Soc. America Mem. 73, 259 p.

Gordon, T. M., 1971, Some observations on the formation of wollastonite from calcite and quartz: Canadian Jour. Earth Sci., v. 8, p. 844-851.

Greenwood, H. J., 1963, The synthesis and stability of anthophyllite: Jour. Petrology, v. 4, p. 317-351.

Haas, H., and Holdaway, M. J., 1973, Equilibria in the system Al_2O_3-SiO_2-H_2O involving the stability limits of pyrophyllite: Am. Jour. Sci., v. 273, p. 449-464.

Helgeson, H. C., Delaney, J. M., Nesbitt, H. W., and Bird, D. K., 1978, Summary and critique of the thermodynamic properties of rock-forming minerals: Am. Jour. Sci., v. 278-A, p. 1-229.

Helgeson, H. D., and Kirkham, D. H., 1974, Theoretical prediction of the thermodynamic behavior of aqueous electrolytes at high pressures and temperatures: I. Summary of the thermodynamic/electrostatic properties of the solvent: Am. Jour. Sci., v. 274, p. 1089-1198.

Helgeson, H. D., Kirkham, D. H., and Flowers, G. C., 1981, Theoretical prediction of the thermodynamic behavior of aqueous electrolytes at high pressures and temperatures: IV. Calculations of activity coefficients, osmotic coefficients and apparent molal and standard and relative partial molal properties to 600°C and 5 kb: Am. Jour. Sci., v. 281, p. 1249-1516.

Holdaway, M. J., 1971, Stability of andalusite and the aluminum silicate phase diagram: Am. Jour. Sci., v. 271, p. 97-131.

Holdren, G. R., and Berner, R. A., 1979, Mechanism of feldspar weathering-I. Experimental studies: Geochim. et Cosmochim. Acta, v. 43, p. 1161-1171.

Hunt, J. A., and Kerrick, D. M., 1977, The stability of sphene: Experimental redetermination and geologic implications: Geochim. et Cosmochim. Acta, v. 41, p. 279-288.

Hurlbut, C. S., 1956, Muscovite from Methuen Township, Ontario: Am. Mineralogist, v. 41, p. 892-898.

Ildefonse, J.-P., and Gabis, V., 1976, Experimental study of silica diffusion during metasomatic reactions in the presence of water at 550° and 1000 bars: Geochim. et Cosmochim. Acta, v. 40, p. 297-303.

Jaeger, J. C., 1957, The temperature in the neighborhood of a cooling intrusive sheet: Am. Jour. Sci., v. 255, p. 306-318.

———— 1959, Temperatures outside a cooling intrusive sheet: Am. Jour. Sci., v. 257, p. 44-54.

Kerrick, D. M., 1968, Experiments on the upper stability limit of pyrophyllite at 1.8 kilobars and 3.0 kilobars water pressure: Am. Jour. Sco., v. 266, p. 204-214.

———— 1972, Experimental determination of muscovite + quartz stability with $P_{H_2O}<P_{TOTAL}$: Am. Jour. Sci., v. 272, p. 946-958.

Kridelbaugh, S. J., 1973, The kinetics of the reaction: Calcite + quartz = wollastonite + carbon dioxide at elevated temperatures and pressures: Am. Jour. Sci., v. 273, p. 757-777.

Lasaga, A. C., 1981a, Rate laws of chemical reactions, *in* Lasaga, A. C., and Kirkpatrick, R. J., eds., Kinetics of Geochemical Processes, Reviews in Mineralogy, v. 8: Washington D.C., Mineralog. Soc. America, p. 1-68.

———— 1984, Chemical kinetics of water-rock interactions: Jour. Geophys. Research, v. 89, p. 4009-4025.

Lasaga, A. C., and Blum, A. E., 1986, Surface chemistry, etch pits, and mineral-water reactions: Geochim. et Cosmochim. Acta, v. 50, p. 2363-2379.

Li, Y-H., and Gregory, A., 1974, Diffusion of ions in sea water and in deep-sea sediments: Geochim. et Cosmochim. Acta, v. 38, p. 703-714.

Luth, W. C., 1974, Analysis of experimental data on alkali feldspars; unit cell parameters and solvi, *in* MacKenzie, W. S., and Zussman, J., eds., The Feldspars: Manchester, Manchester Univ. Press, p. 249-296.

Martin, B., and Fyfe, W. S., 1970, Some experimental and theoretical observations on the kinetics of hydration reactions with particular reference to serpentinization: Chem. Geology, v. 6, p. 185-202.

Matthews, A., 1980, Influences of kinetics and mechanism in metamorphism: A study of albite crystallization: Geochim. et Cosmochim. Acta, v. 44, p. 387-402.

Nigrini, A., 1970, Diffusion in rock alteration systems: I. Prediction of limiting ionic conductances at elevated temperatures: Am. Jour. Sci., v. 269, p. 65-91.

Perry, D. L., Tsao, L., and Gaugler, K. A., 1983, Surface study of HF/H_2SO_4-treated feldspar using Auger electron spectroscopy: Geochim. et Cosmochim. Acta, v. 47, p. 1289-1291.

Robie, R. A., Hemingway, B. S., and Fisher, J. R., 1978, Thermodynamic properties of minerals and related substances at 298.15 K and 1 bar (10^5 pascals) pressure and at higher temperatures: U.S. Geol. Survey Bull. 1452, 456 p.

Robie, R. A., Hemingway, B. S. and Wilson, W. H., 1976, The heat capacities of calorimetry conference copper and of muscovite $(KAl_2(AlSi_3)O_{10}(OH)_2$, pyrophyllite $Al_2Si_4O_{10}(OH)_2$, and illite $K_3(Al_7Mg)(Si_{14}Al_2)O_{40}(OH)_8$ between 15 and 375 K and their standard entropies at 298.15 K: U.S. Geol. Survey, Jour. Research, v. 4, p. 631-644.

Rubie, D. C., and Thompson, A. B., 1985, Kinetics of metamorphic reactions at elevated temperatures and pressures: an appraisal of available experimental data, *in* Thompson, A. B., and Rubie, D. C., eds., Advances in Physical Geochemistry, v. 4, Metamorphic Reactions—Kinetics, Textures, and Deformation: New York, Springer-Verlag, p. 27-79.

Schramke, J. A., ms, 1984, The Kinetics of Metamorphic Hydration-Dehydration Reactions: Ph.D. dissert., The Pennsylvania State Univ., 209 p.

Sipling, P. J., and Yund, R. A., 1974, Kinetics of Al/Si disordering in alkali feldspars, *in* Hoffman, A. W., Giletti, B. J., Yoder, H. S., and Yund, R. A., eds., Geochemical Transport and Kinetics: Washington D.C., Carnegie Inst. of Washington, p. 173-184.

Stewart, D. B., and Wright, T. L., 1974, Al/Si order and symmetry of natural alkali feldspars, and the relationship of strained cell parameters to bulk composition: Bull. Soc. franc. Mineralogie Crystallographie, v. 97, p. 356-377.

Storre, B., and Karotke, E., 1971, An experimental determination of the upper stability limit of muscovite + quartz in the range 7-20 kb water pressure: Neues Jahrb. Mineralogie Monatsh., p. 237-240.

Tanner, S. B., Kerrick, D. M., and Lasaga, A. C., 1985, Experimental kinetic study of the reaction: calcite + quartz ⇄ wollastonite + carbon dioxide, from 1 to 3 kilobars and 500° to 850°C: Am. Jour. Sci., v. 285, p. 577-620.

Todheide, K., 1972, Water at high temperatures and pressures, *in* Franks, F., ed., Water, A Comprehensive Treatise: New York, Plenum Press, p. 463-514.

Turner, F. J., 1981, Metamorphic Petrology: Mineralogical, Field and Tectonic Aspects: New York, McGraw-Hill, 524 p.

Wegner, W. W., and Ernst, W. G., 1983, Experimentally determined hydration and dehydration reaction rates in the system $MgO-SiO_2-H_2O$: Am. Jour. Sci., v. 283-A, p. 151-180.

Wood, B. J., and Walther, J. V., 1983, Rates of hydrothermal reactions: Science, v. 222, p. 413-415.